

Central Lancashire Online Knowledge (CLoK)

Title	A review on the two-phase pressure drop characteristics in helically coiled tubes
Type	Article
URL	https://clock.uclan.ac.uk/13844/
DOI	##doi##
Date	2016
Citation	Fsadni, A orcid iconORCID: 0000-0003-3047-2714 and Whitty, J orcid iconORCID: 0000-0003-1002-5271 (2016) A review on the two-phase pressure drop characteristics in helically coiled tubes. Applied Thermal Engineering, 103 . pp. 616-638. ISSN 1359-4311
Creators	Fsadni, A and Whitty, J

It is advisable to refer to the publisher's version if you intend to cite from the work. ##doi##

For information about Research at UCLan please go to <http://www.uclan.ac.uk/research/>

All outputs in CLoK are protected by Intellectual Property Rights law, including Copyright law. Copyright, IPR and Moral Rights for the works on this site are retained by the individual authors and/or other copyright owners. Terms and conditions for use of this material are defined in the <http://clock.uclan.ac.uk/policies/>

Manuscript details

Manuscript number HMT_2016_438

Title A review on the two-phase pressure drop characteristics in helically coiled tubes

Article type Review Article

Abstract Due to their compact design, ease of manufacture and enhanced heat transfer and fluid mixing properties, helically coiled tubes are widely used in a variety of industries and applications. In fact, helical tubes are the most popular from the family of coiled tube heat exchangers. This review summarises and critically reviews the studies reported in the pertinent literature on the pressure drop characteristics of two-phase flow in helically coiled tubes. The main findings and correlations for the frictional two-phase pressure drops due to: steam-water flow boiling, R-134a evaporation and condensation, air-water two-phase flow and nanofluid flows are reviewed. Therefore, the purpose of this study is to provide researchers in academia and industry with a practical summary of the relevant correlations and supporting theory for the calculation of the two-phase pressure drop in helically coiled tubes. A significant scope for further research was also identified in the fields of: air-water bubbly flow and nanofluid two phase and three-phase flows in helically coiled tubes.

Keywords Two-phase flow; curved tubes; frictional pressure drop; flow boiling; nanofluids

Corresponding Author Andrew Fsadni

Corresponding Author's Institution University of Central Lancashire

Order of Authors Andrew Fsadni, Justin Whitty

Suggested reviewers Mohamed Basuny, Bengt Sunden, Harry Edmar Schulz

Submission files included in this PDF

File Type	File Name
Cover Letter	Cover Letter_A Fsadni_08__02_16.pdf
Conflict of Interest	Author Declaration_A Fsadni_08_02_16.pdf
Title page with author details	Title Page_Review Paper_Helical Coils_Pressure Drop_08_02_16.pdf
Highlights	Highlights_Review Paper_Helical Coils_Pressure Drop_08_02_16.pdf
Manuscript	Manuscript_Review paper_Pressure Drop_Helical Coils_08_02_16.pdf

To view all the submission files, including those not included in the PDF, click on the manuscript title on your EVISE Homepage, then click 'Download zip file'.

Room: KM 124
School of Engineering
University of Central Lancashire,
Preston
UK, PR1 2HE

The Editor,
International Journal of Heat and Mass Transfer,
Elsevier Publishing

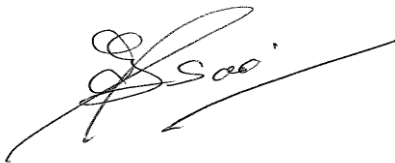
8th February 2016

Dear Prof. Rose,

I would like to submit the attached manuscript entitled: '*A review on the two-phase pressure drop characteristics in helically coiled tubes*' for publication in the International Journal of Heat and Mass Transfer. This research complements our earlier paper entitled: '*A review on the two-phase heat transfer characteristics in helically coiled tube heat exchangers*'. For the purposes of the current submission, I have selected the Elsevier 'Your Paper Your Way' submission process.

I thank you for taking the time to consider this request and I look forward to hearing from you in due course.

Yours sincerely,

A handwritten signature in black ink, appearing to read 'A. Fsadni', with a long horizontal line extending to the right.

Dr. Andrew M. Fsadni
PhD, MSc, MBA, BEng (Hons), EUR ING, FHEA, CEng, MIMechE
Lecturer, School of Engineering,
University of Central Lancashire, UK

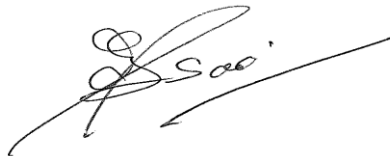
Author Declaration

I wish to confirm that there are no known conflicts of interest associated with this publication and there has been no significant financial support for this work that could have influenced its outcome.

I confirm that Dr Justin P.M. Whitty and the undersigned are the sole authors of the manuscript and therefore, there are no other persons who satisfied the criteria for authorship but are not listed.

I confirm that, due consideration has been given to the protection of intellectual property associated with this work and that there are no impediments to publication, including the timing of publication, with respect to intellectual property. In so doing, I confirm that I have followed the regulations of my institution concerning intellectual property.

I understand that as a Corresponding Author, I am the sole contact for the Editorial process. I confirm that I have provided a current, correct email address which is accessible by myself as the Corresponding Author and which has been configured to accept emails from The International Journal of Heat and Mass Transfer.

A handwritten signature in black ink, appearing to read 'A. M. Fsadni', with a long horizontal stroke extending to the right.

Dr Andrew M. Fsadni

08th February 2016

Title: A review on the two-phase pressure drop characteristics in helically coiled tubes

Authors: Andrew Michael Fsadni*, Justin P.M. Whitty

*Corresponding author

Contact details:

Address: University of Central Lancashire, School of Engineering, Rm. KM124, Preston, UK, PR1 2HE

Email: afsadni@uclan.ac.uk

Tel: +44 1772893812

Highlights

- Detailed review on the two-phase pressure drop characteristics and correlations
- Impact of curvature on the flow boiling frictional pressure drop is not significant
- Nanofluids' impact on the pressure drop is significant
- There is a significant gap in literature in the field of frictional drag reduction

A review on the two-phase pressure drop characteristics in helically coiled tubes

Abstract

Due to their compact design, ease of manufacture and enhanced heat transfer and fluid mixing properties, helically coiled tubes are widely used in a variety of industries and applications. In fact, helical tubes are the most popular from the family of coiled tube heat exchangers. This review summarises and critically reviews the studies reported in the pertinent literature on the pressure drop characteristics of two-phase flow in helically coiled tubes. The main findings and correlations for the frictional two-phase pressure drops due to: steam-water flow boiling, R-134a evaporation and condensation, air-water two-phase flow and nanofluid flows are reviewed. Therefore, the purpose of this study is to provide researchers in academia and industry with a practical summary of the relevant correlations and supporting theory for the calculation of the two-phase pressure drop in helically coiled tubes. A significant scope for further research was also identified in the fields of: air-water bubbly flow and nanofluid two phase and three-phase flows in helically coiled tubes.

Keywords: *Two-phase flow; curved tubes; frictional pressure drop; flow boiling; nanofluids*

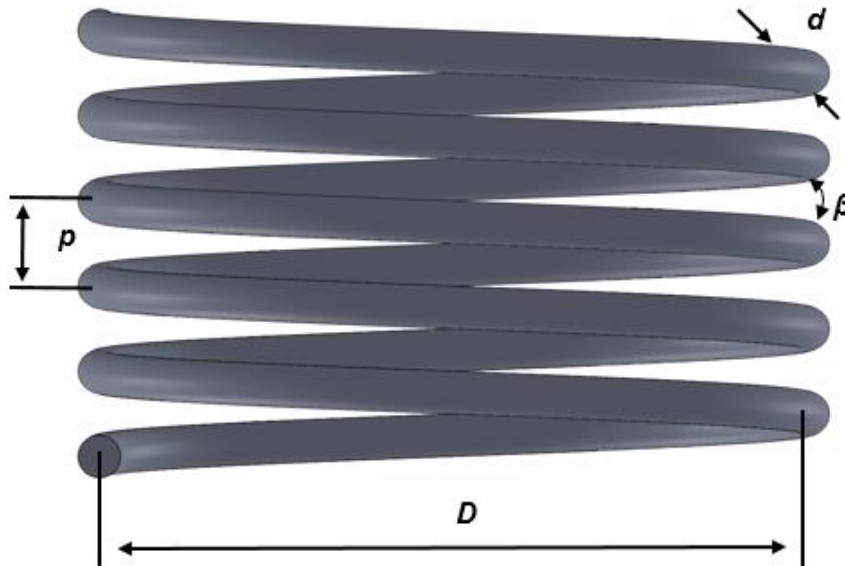
1. Introduction

Due to their compact design, ease of manufacture and high efficiency in heat and mass transfer, helically coiled tubes are widely used in a number of industries and processes such as in the food, nuclear, aerospace and power generation industries and in heat recovery, refrigeration, space heating and air-conditioning processes. Due to the formation of a secondary flow, which inherently enhances the mixing of the fluid, helically coiled tube heat exchangers are known to yield improved heat transfer characteristics when compared to straight tube heat exchangers. The secondary flow is perpendicular to the axial fluid direction and reduces the thickness of the thermal boundary layer. Goering et al. [1] estimated the secondary flow to account for circa 16-20% of the mean fluid flow velocity. This phenomenon finds its origins in the centrifugal force due to the curvature of the coil structure and is more evident with laminar flow due to the limited fluid mixing in straight tube laminar flow [2,3]. However, for single and two-phase flows, the secondary flow could also result in an undesirable increase in the frictional pressure drop over that of straight tubes. For air-water two-phase flow in helically coiled tubes, Akagawa et al. [4] reported frictional pressure drops in the range of 1.1 to 1.5 times greater than those in straight tubes, *ceteris paribus*. Therefore, the performance of helical coils is also a function of the geometry and design parameters such as the tube diameter and the pitch (Fig. 1) as well as the resultant pressure drop. Through their study on the investigation of the heat transfer characteristics with the addition of multi-walled carbon nanotubes nanoparticles to oil, Fakoor-Pakdaman et al. [5] reported their results in terms of the Performance Index (*PI*), given in Eq. (1). This captures the simultaneous effects of heat transfer and two-phase pressure drop with the use of nanofluids and helical tubes on the overall performance of the heat exchanger. When the performance index is greater than unity, the *PI* implies that the benefits gained through enhanced heat transfer coefficients outweigh the effects of larger pressure drops as a result of the nanoparticles and helical tubes.

$$\eta = \frac{\frac{h^*}{h_{st}}}{\frac{\Delta P^*}{\Delta P_{st}}} \quad (1)$$

49
50
51
52
53
54

where h^* is the mean heat transfer coefficient after the application of enhancement techniques, h_{st} is the mean heat transfer coefficient in a straight tube with the base fluid only, ΔP^* is the mean pressure drop after the application of enhancement techniques and ΔP_{st} is the mean pressure drop inside a straight tube with the base fluid only.



55
56
57

Figure 1: Schematic representation of helical pipe characteristics

58
59
60
61
62
63
64
65
66
67
68
69
70
71
72
73

The pertinent literature, presents a considerable number of widely cited studies on the pressure drop for single-phase flow in helically coiled tubes [6,7]. A lesser number of studies have investigated the two-phase pressure drop characteristics in helically coiled tubes. Whilst being more relevant to real-life engineering systems, when compared to single-phase flow, two-phase flow is significantly more complex due to the combination of the three forces governing the flow regime, these being the: inertia, liquid gravity and centrifugal forces [8]. Numerous studies investigated the two-phase frictional pressure drop with steam-water flow boiling [9,10], R-134a refrigerant flows [11,12] and air-water flows [4] whilst more recently, a number of authors investigated the application of nanofluids [13,14] in helically coiled tubes through experimental and computational studies. Mandal and Das [15] and Murai et al. [16] reported that the phase with the lower density is subjected to a smaller centrifugal force which forces the lighter phase to shift towards the inner side of the coil's wall. However, Saffari et al. [17] reported that for bubbly flows at elevated Reynolds numbers and characterised by small bubble diameters ($b < 0.5\text{mm}$), the enhanced fluid mixing could result in a quasi-homogenous distribution of the secondary phase. This draws an analogy to similar investigations with nanofluids where no significant phase separation was reported [18].

74
75
76
77
78
79
80
81
82

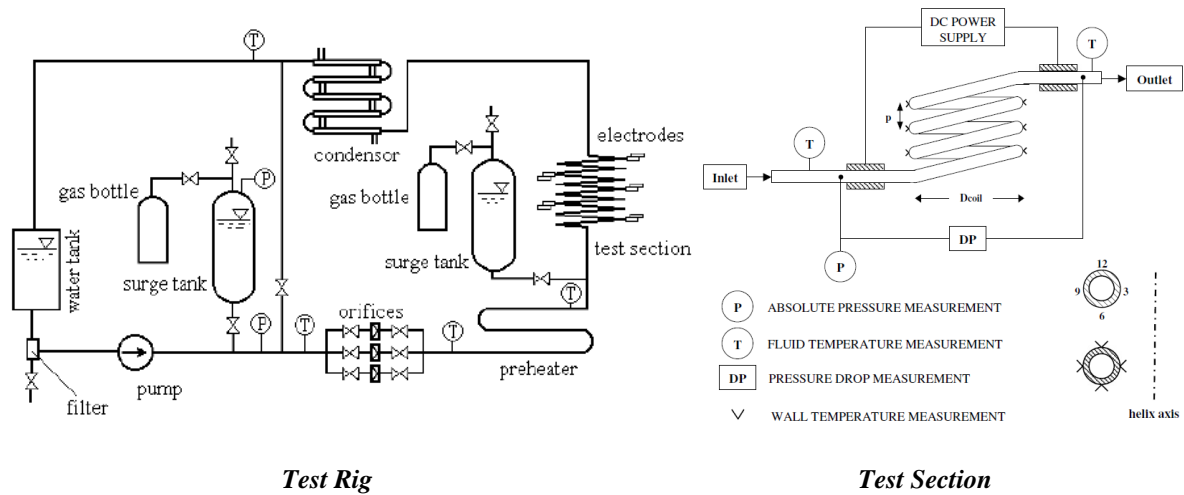
A recent development in the field of bubbly air-water two-phase flow has resulted in the injection of microbubbles in the flow to achieve a reduction in the system frictional pressure drop. Hitherto, this research has focused on the injection of air bubbles over flat plates and in straight tubes with a minimal consideration for the investigation of the pressure drop reduction in coiled tubes. When investigating the drag reduction inside a channel Nouri et al. [19] reported that bubble injection can be used to decrease the flow transfer costs. In fact, they reported a 35% reduction in the pressure drop in turbulent upward pipe flow with the maximum experimental volumetric void fraction of 9%. This is attributed to the congregation of the larger bubbles at the pipe wall. To the best of the authors' knowledge, the sole investigation with

83 coiled tubes was done by Saffari et al. [17] who reported an increase in the magnitude of drag
 84 reduction with increasing volumetric void fraction and decreasing Reynolds and Dean
 85 Numbers. These conclusions contrast to the findings reported by the majority of investigations
 86 on air-water bubbly flows, where two-phase pressure drop multipliers in excess of unity were
 87 reported [20, 8]. The pertinent literature also presents some controversy through conflicting
 88 results on the impact of nanoparticles on the frictional pressure drop in helically coiled tubes.
 89 In fact, whereas the majority of investigations reported a rise in the pressure drop with the
 90 particle concentration [21, 22], some investigations concluded that the opposite effect could
 91 occur [23].

92 Naphon and Wongwiset [24] briefly reviewed the single and two-phase flow and
 93 pressure drop characteristics in curved tubes. However, their review was principally focused
 94 on the single-phase flow characteristics and hence they failed to adequately review the pertinent
 95 literature for two-phase flow. Therefore, to the best of the authors' knowledge the open
 96 literature does not present comprehensive reviews on the pressure drop characteristics of two-
 97 phase flow in helically coiled tube heat exchangers. The current study will therefore present a
 98 review of the pertinent literature on the two-phase frictional pressure drop characteristics and
 99 correlations in helically coiled tubes. It is the authors' hope that this review will be useful to
 100 both academics and industry based engineers through the provision of a comprehensive report
 101 on the relevant current knowledge and controversies in literature. The present study will also
 102 identify areas for further research.

103
 104 *1.1 Research Methods*

105
 106 Experimental and numerical methods were used to investigate the pressure drop characteristics
 107 in helically coiled tubes. Fig. 2 presents a schematic diagram of the test facility developed by
 108 Guo et al. [25] and Cioncolini et al. [26] for the investigation of the steam-water flow boiling
 109 pressure drop in helically coiled tubes at varying operating system parameters such as



110
 111
 112
 113
 114
 115
 116
 117
 118
 119
 120
 121
 122

Figure 2: Schematic diagram of the typical experimental test rig for the investigation of the flow boiling two-phase pressure drop in helically coiled tubes (Guo et al. (2001b) [25] Fig. 1) and the typical test section (Cioncolini et al. [26], Fig. 2)

the pressure, heat and mass fluxes. This setup is typical for most experimental studies in this field of study. An experimental uncertainty of 2.5% was reported by Cioncolini et al. for their two-phase pressure drop measurements.

As illustrated in Fig. 2, the typical experimental setup for the investigation of the flow boiling two-phase pressure drop characteristics in helically coiled tubes included a centrifugal

123 pump for maintaining the system mass flow rate. Before entering the test section, the working
 124 fluid was heated to a subcooled state through the use of the pre-heater. The system bulk fluid
 125 flow rates were typically controlled by the system circulation pump. Stainless steel [25,27, 28]
 126 was used for the test section, which was thermally insulated to minimise the heat losses to the
 127 environment. The majority of the studies reviewed in this paper used the electrical direct
 128 heating method to heat the test section whilst, armoured K-type thermocouples were typically
 129 used to measure the bulk fluid temperature along the test section. K-type thermocouples,
 130 welded to the outside surface of the tube, were also used to measure the tube's wall temperature.
 131 These thermocouples were electrically insulated in order to avoid the effects of the heating
 132 electrical currents on it. Pressure sensors, installed at the return and flow ends of the helically
 133 coiled tube, measured the total two-phase pressure drop whilst a water cooled condenser
 134 condensed the steam or refrigerant vapour after the test section. The signals from the various
 135 measuring sensors were channelled to a data acquisition system for data monitoring and
 136 processing purposes.

137 All the numerical investigations reviewed in the current study were developed through
 138 the use of a commercially available computational fluid dynamics package, namely ANSYS
 139 Fluent [22, 29]. The majority of authors validated their experimental and numerical methods
 140 through the comparison of the single-phase frictional pressure drop data with widely cited
 141 single-phase correlations for helically coiled tubes, such as those given by Ito [30] and Mishra
 142 and Gupta [31].

144 2. Flow boiling heat transfer coefficient

146 2.1. Steam and Water

147
 148 A number of correlations are presented in the open literature for the calculation of the flow
 149 boiling pressure drop multiplier in helically coiled tubes for a wide range of system parameters.
 150 The reviewed correlations are summarised in Table 1 according to the key parameters
 151 governing their applications. The total two-phase pressure drop can be broken down into three
 152 component pressure drops these being the frictional, gravitational and the momentum pressure
 153 drops (Eqs.2-5) [32]. Many researchers have presented the two-phase frictional pressure drop
 154 as a function of the pressure drop multiplier and the single-phase frictional pressure drop as
 155 given in Eq. (3).

$$157 \Delta P_{total,TP} = \Delta P_{f,TP} + \Delta P_{grav} + \Delta P_{acc} \quad (2)$$

$$159 \Delta P_{f,TP} = \Delta P_l \phi_l^2 \quad (3)$$

160
 161 where $\Delta P_{f,TP}$ is the two-phase flow frictional pressure drop of helical coils, and ΔP_l is the
 162 frictional pressure drop of the single-phase fluid flowing through the tube with the assumption
 163 that only liquid flows through the tube. Many authors have used the single-phase friction factor
 164 numerical model given by Ito [6] to calculate the latter pressure drop.

$$166 \Delta P_{grav} = \left[\frac{gH}{x_{exit} - x_{inlet}} \right] \left[\frac{\ln \left(1 + x \left(\frac{\rho_l}{\rho_g} - 1 \right) \right)}{\left(\frac{1}{\rho_g} - \frac{1}{\rho_l} \right)} \right]_{exit} - \left[\frac{gH}{x_{exit} - x_{inlet}} \right] \left[\frac{\ln \left(1 + x \left(\frac{\rho_l}{\rho_g} - 1 \right) \right)}{\left(\frac{1}{\rho_g} - \frac{1}{\rho_l} \right)} \right]_{in} \quad (4)$$

$$168 \Delta P_{acc,TP} = G^2 \left\{ \left[\frac{1-x}{\rho_l} + \frac{x}{\rho_g} \right]_{exit} - \left[\frac{1-x}{\rho_l} + \frac{x}{\rho_v} \right]_{in} \right\} \quad (5)$$

170 There appears to be a general agreement amongst the pertinent studies reviewed that
171 the two-phase flow boiling frictional pressure drop increases with the vapour quality and mass
172 flux whilst it decreases with higher system pressures. The curvature ratio does not appear to
173 have a significant influence on the two-phase flow boiling frictional pressure drop multiplier
174 whilst there is some controversy surrounding the influence of the coil orientation and heat flux.
175 Over the past 50 years, the application of numerical models to predict the flow boiling frictional
176 pressure drop in coiled tubes has highlighted the general difficulty in predicting the flow
177 characteristics of two-phase flow. Therefore, many authors have presented their own empirical
178 or semi-empirical models, or correlated existing models to fit their experimental data. The
179 earliest investigations on the flow boiling frictional pressure drop in helically coiled tubes [10,
180 28, 33] correlated the experimental data with well-known numerical models for the two-phase
181 frictional pressure drop multiplier for straight tubes as given by Lockhart and Martinelli [34],
182 Martinelli and Nelson [35] and Chen [36]. The latter are typically a function of the Lockhart
183 and Martinelli parameter, which, in turn, is a function of the vapour quality and the densities
184 and viscosities of the liquid and gas phases.

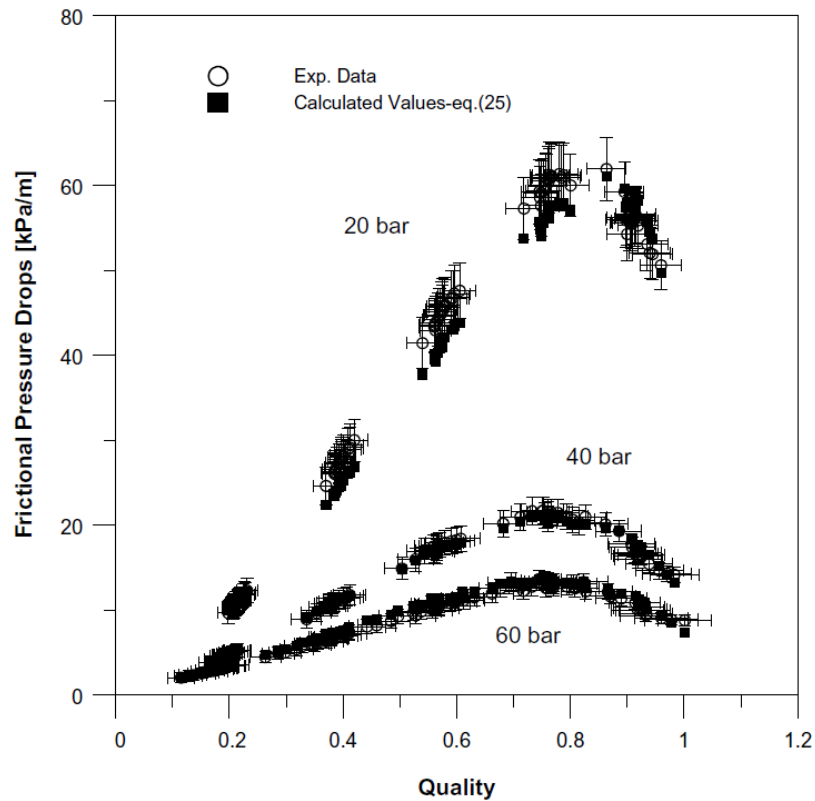
185 Kozeki et al. [28] reported that at the flow boiling region, the frictional pressure drop
186 was circa 70 percent larger than that predicted by the Martinelli and Nelson numerical model
187 for two-phase flow in straight tubes. The higher frictional pressure drop was attributed to the
188 secondary flow phenomenon in the vapour core region where the largest influence was
189 recorded at low pressures and high Reynolds numbers. Such results are in agreement with more
190 recent studies reported by Guo et al. [37] and Santini et al. [38] who concluded that the
191 frictional pressure drop decreases with higher system pressures (Fig.3). This is due to the
192 resultant lower specific volume which in turn yields a lower mixture velocity. Nariai et al. [10]
193 also reported that the effects of the flow boiling phenomena on the frictional pressure drop are
194 not distinct in the fluid conditions.

195 The influence of the vapour quality on the frictional pressure drop does not appear to
196 be uniform over the complete vapour quality range. Guo et al. [37] and Zhao et al. [27] reported
197 that at vapour qualities below 0.3, the frictional pressure drop increased significantly with the
198 vapour quality whilst at higher qualities this increase was less significant. Santini et al. also
199 reported that the increase in the frictional pressure drop stopped at a vapour quality of 0.8 and
200 subsequently decreased as the quality approached unity. They attributed this phenomenon to
201 the annular flow regime where the liquid film becomes too thin to maintain the interface waves.
202 No other authors have reported similar results for helically coiled tubes and therefore, the latter
203 results can be classified as indeterminate and hence, present ample scope for further
204 investigations.

205 Bi et al. [32] and Zhao et al. [27] are the sole authors to report that the heat flux does
206 not have a significant impact on the frictional pressure drop. However, more recently,
207 Cioncolini et al. [26] reported that the heating effects resulted in an influence on the frictional
208 pressure drop and hence, their correlation for the frictional pressure drop multiplier is also a
209 function of the system heat flux. They attributed this influence to the interface between the
210 liquid film and the vapour core being dependent on the evaporation and nucleation processes.

211 Bi et al. [32] and Guo et al. [37] are the sole authors who investigated the flow boiling
212 frictional pressure drop as a function of the coil orientation. However, whilst the former
213 reported that the coil orientation had no significant impact on the two-phase frictional pressure
214 drop, the latter reported distinctly different results. Guo et al. reported that the horizontal coils
215 resulted in the smallest frictional pressure drop whilst the 45 degree, downwards inclined coils
216 resulted in the largest measured pressure drop (70% higher than that measured for the
217 horizontal orientation). The frictional pressure drop for the vertical coil was between that
218 measured for the horizontal and the inclined orientations. Guo et al. attributed these results to
219 the variation in the secondary flow regime with the tube orientation. The authors of the present

220 study cannot adequately address the differences in these two results as the system parameters
 221 for both studies were distinctly similar. However, drawing on the conclusions reported by
 222 Santini et al. [38] regarding the influence of the system pressure on the pressure drop, the
 223 significantly higher system pressure used in Bi et al.'s investigation could suggest that at high
 224 system pressures, the flow boiling frictional pressure drop is quasi-independent of the coil
 225 orientation.
 226



227
 228 **Figure 3: Experimental and predicted (Equation for $\Delta P_{f,TP}$ in Table 1) two-phase flow frictional pressure**
 229 **drop with system pressure and vapour quality at a constant mass flux of $600\text{kg/m}^2\text{s}$ (Santini et al. [38], Fig.**
 230 **7)**
 231

Correlations derived from the widely used two-phase flow pressure drop correlations for straight tubes ($P < 3.5\text{MPa}$ & $d \geq 12\text{mm}$)				
Authors	Helical coil design parameters	Principal experimental parameters	Steam quality	Main conclusions, proposed correlation and mean error
Owhadi et al. (1968) [33]	15.9mm OD 12.5mm ID 250 < D < 527 Vertical	0.024 < δ < 0.05 $P = 0.1\text{MPa}$ 60 < q < 256 0.0097 < \dot{m} < 0.039 80 < G < 315	0.5 < x < 1	Data has resulted in a considerable scatter. In general, it agreed with the Lockhart and Martinelli [34] equation for a straight tubes $\phi_{l,tt}^2 = 1 + \frac{C}{\chi_{tt}} + \frac{1}{\chi_{tt}^2}$ where C is a constant dependent on the gas and liquid Reynolds numbers $\chi_{tt} = \left(\frac{1-x}{x}\right)^{0.9} \left(\frac{\rho_g}{\rho_l}\right)^{0.5} \left(\frac{\mu_l}{\mu_g}\right)^{0.1}$
Kozeki (1970) [28]	21.7mm OD 628 < D < 682m m	0.032 < δ < 0.035 0.5 < P < 2.1MPa 151 < q < 348 161 < G < 486	0 < x < 1	Pressure drop is greater than that for a straight tube and it increases with vapour quality and mass flux..

	Vertical			<p>Numerical model based on the Martinelli and Nelson prediction for two-phase flow in straight tubes</p> $\phi_{g,tt}^2 = 0.895 + (\chi_{tt} + 0.076)^{0.875} + 1.21 * 10^{-0.334(\log\chi_{tt}+0.668)^2}$ <p>where:</p> $\phi_{ltt} = \frac{\phi_{g,tt}}{\chi_{tt}^{0.875}}$
Nariai et al. (1982) [10]	14.3&20mm ID D=595mm Vertical	0.024< δ <0.034 2<P<3.5MPa 0.7E5<q<1.8E5 150<G<850	0.1<x<0.9	<p>Pressure drop increases with mass flux and vapour quality.</p> <p>Martinelli and Nelson [35] prediction for straight tubes:</p> $\Delta P_{f,TP} = R_{MN} \Delta P_l$ $R_{MN} = (1-x)^{1.75} \phi_{l,tt}^2 = \phi_l^2(P, x)$ <p>Experimental values for ϕ_l^2 were given in table as a function of the system pressure, P and quality, x.</p> <p>Kozeki [28] prediction (better fit)</p> $\phi_{g,tt}^2 = 0.895 + (\chi_{tt} + 0.076)^{0.875} + 1.21 * 10^{-0.334(\log\chi_{tt}+0.668)^2}$ <p>where:</p> $\phi_{ltt} = \frac{\phi_{g,tt}}{\chi_{tt}^{0.875}}$ <p>(30%)</p>
Guo et al. (2001) [37]	10&11mm ID D=132&256 mm Horizontal/Vertical and Inclined	0.043< δ <0.076 3<P<3.5MPa 0<q<540 150<G<1760	-0.01<x<1.2	<p>The coil orientation has a significant influence on the frictional pressure drop. Pressure drop is also a function of the system pressure and mass quality.</p> <p>Based on Chen's [36] correlation for straight tubes:</p> $\phi_l^2 = \psi_1 \psi \left[1 + x \left(\frac{\rho_l}{\rho_g} - 1 \right) \right]$ <p>where: for $G \leq 1000$</p> $\psi = 1 + \frac{x(1-x) \left(\frac{1000}{G} - 1 \right) \left(\frac{\rho_l}{\rho_g} \right)}{1 + x \left(\frac{\rho_l}{\rho_g} - 1 \right)}$ <p>for $G > 1000$</p> $\psi = 1 + \frac{x(1-x) \left(\frac{1000}{G} - 1 \right) \left(\frac{\rho_l}{\rho_g} \right)}{1 + (1-x) \left(\frac{\rho_l}{\rho_g} - 1 \right)}$ $\psi_1 = 142.2 \left(\frac{P}{P_{crit}} \right)^{0.62} \delta^{1.04}$ <p>(±12%)</p>
Correlations for high system pressures based (P>3.5MPa)				
Ruffell (1974) [39]	10.7<ID<18.6 mm	0.0054< δ <0.16 6<P<18MPa 41<q<731 300G<1800	0<x<1	$\phi_l^2 = (1+F) \frac{v_m}{v_l}$ <p>where:</p> $F = \sin \left(\frac{1.16G}{1000} \right) \left\{ 0.875 - 0.314y - \frac{0.74G}{1000} (0.152 - 0.07y) - x \left(\frac{0.155G}{1000} + 0.7 - 0.19y \right) \right\} \left\{ 1 - 12(x - 0.3)(x - 0.4)(x - 0.5)(x - 0.6) \right\}$

				$y = \frac{D}{100d}$
Unal et al. (1981) [40]	18 mm ID 700&1500mm =D Vertical	0.0054< δ <0.022 14.7<P<20.2MPa 41<q<731 112<G<1829	0.08<x<1	$\Delta P_{f,TP} = \frac{2(1 + b_1 b_2) f_l G^2}{d \rho_l}$ <p>where:</p> $b_1 = 3850x^{0.01} Pr^{-1.515} Re_l^{-0.758}$ $b_2 = 1 + Re_l^{0.1} (3.67 - 3.04 P_b)^{(-0.014\delta^{-1}) - (2\delta^{-1})}$ <p>where:</p> $P_b = \frac{P}{P_{crit}}$ $f_l = 0.076 Re^{-0.25} + 0.00725 \delta^{0.5} \quad [6]$ <p>(±20%)</p>
Chen and Zhou (1981) [41]	18 mm ID 235, 446,907 mm=D Vertical	0.02< δ <0.076 4.2<P<22MPa 400<G<2000	0<x<1	$\Delta P_{f,TP} = \xi \Delta P_{st}$ <p>where:</p> $\xi = 2.06 \delta^{0.05} Re_{TP}^{-0.025} \left[1 + VF \left(\frac{\rho_g}{\rho_l} - 1 \right) \right]^{0.8} \left[1 + x \left(\frac{\rho_l}{\rho_g} - 1 \right) \right]^{1.8} \left[1 + VF \left(\frac{\mu_g}{\mu_l} - 1 \right) \right]^{0.2}$
Santini et al. (2008) [38]	12.53 mm ID D=1000mm Vertical	$\delta=0.019$ 1.1<P<6.3MPa 50<q<200 192<G<824	0<x<1	<p>Frictional pressure drop increases with the vapour quality and mass flux whilst it decreases with the system pressure.</p> $\Delta P_{f,TP} = K \left(\frac{G^{1.91} v_m}{d^{1.2}} \right) \Delta z$ <p>where:</p> $K(x) = -0.0373x^3 + 0.0387x^2 - 0.00479x + 0.0108$ <p>(RMS = 6.2)</p>
Correlations for large tube diameters ($d \geq 12\text{mm}$)				
Guo et al. (1994) [42]	20 mm ID 240, 480,960 mm=D Horizontal	0.021< δ <0.083 1.5 <P<3MPa 150<G<1400	0<x<0.8	$\phi_l^2 = 1 + (4.25 - 2.55x^{1.5})G^{0.34}$
Correlations for small tube and helix diameters ($d < 12\text{mm}$)				
Kubair (1986) [43]	6.4&6.5mm ID 110<D<177 Laminar & Turbulent Vertical	0.037< δ <0.056 8<P<16kPa 6<q<80 0.0028< \dot{m} <0.016 1300<Re<5200	0.2<x<0.8	<p>Frictional pressure drop is larger than that for straight tubes.</p> <p>No correlation provided.</p>
Bi et al. (1994) [32]	10&12mm ID D=115mm Horizontal& Vertical	0.087< δ <0.104 4<P<14MPa 0<q<750 400<G<2000	0<x<1	<p>Coil orientation has no significant effect on the two-phase frictional pressure drop. The two-phase frictional pressure drop was not influenced by the conditions of the thermodynamic system i.e. adiabatic or electrically heated tubes.</p> $\phi_l^2 = 1 + \left[\frac{\rho_l}{\rho_g} - 1 \right] [C + x^2]$ <p>where:</p>

				$C = 0.14691x^{1.3297}(1-x)^{0.59884}\delta^{-1.2864}$ <p style="text-align: center;">(±15%)</p>
Ju et al. (2001) [44]	18mm OD D=112mm Turbulent	$\delta=0.161$ $P=3\text{MPa}$ $2500 < Re < 23000$	$0 < x < 1$	$\Delta P_{f,TP} = f \left(\frac{L}{d} \right) \left(\frac{\rho V^2}{2} \right) \left[1 + x \left(\frac{\rho'}{\rho'' - 1} \right) \right] \psi$ <p>where:</p> $\psi = (1.29 + A_n x^n) \left[1 + x \left(\left(\frac{\mu''}{\mu'} \right)^{0.25} - 1 \right) \right]$ <p style="text-align: center;">$A_1=2.19, A_2=-3.61, A_3=7.35, A_4=-5.93$</p>
Zhao et al. (2003) [27]	9mm ID D=292mm Laminar Horizontal	$\delta=0.031$ $0.5 < P < 3.5 \text{ MPa}$ $0 < q < 900$ $236 < G < 943$ $10000 < Re < 80000$	$0.1 < x < 0.2$	<p>Frictional pressure drop is a function of the mass flux, vapour quality and the system pressure. Heat flux has no effect on the pressure drop.</p> $\phi_l^2 = 1 + \left[\frac{\rho_l}{\rho_g} - 1 \right] \left[0.303x^{1.63} (1 - x)^{0.885} Re_l^{0.282} + x^2 \right]$ <p style="text-align: center;">(±12%)</p>
Cioncolini et al. (2008) [26]	4.03&4.98mm ID $130 < D < 376$ Turbulent Vertical Saturated flow boiling	$0.011 < \delta < 0.038$ $120 < P < 660 \text{ kPa}$ $50 < q < 440$ $290 < G < 690$ $10000 < Re < 60000$ $2 < Fr < 14$	$0 < x < 0.9$	<p>Minimal effect of the coil curvature on the frictional pressure drop. Lockhart and Martinelli correlation for straight tubes corrected for heating effects [45]:</p> $\phi_l^2 = \left[1 + \frac{C}{\chi_{tt}} + \frac{1}{\chi_{tt}^2} \right] \left[1 + 0.0044 \left(\frac{q}{G} \right)^{0.7} \right]$ <p style="text-align: center;">(16.7%) Zhao et al. [27]</p> $\phi_l^2 = 1 + \left[\frac{\rho_l}{\rho_g} - 1 \right] \left[0.303x^{1.63} (1 - x)^{0.885} Re_l^{0.282} + x^2 \right]$ <p style="text-align: center;">(16.3%)</p>

Table 1: Review of the experimental studies on the flow boiling frictional pressure drop characteristics of steam-water in helically coiled tubes

2.2. R-134a

The pressure drop characteristics and relevant correlations for flow boiling and condensation of R-134a in helically coiled tube heat exchangers are summarised in Table 2. In contrast to the conclusions made by a number of investigations on steam and water flow boiling, the curvature ratio appears to have some impact on the resultant frictional pressure drop for R-134a flow in non-miniature helically coiled tubes. The pertinent investigations have also concluded that the frictional pressure drop increases with higher vapour qualities and refrigerant mass fluxes, whilst the tube orientation has no significant impact on the pressure drop. The total two-phase pressure drop for the flow boiling of R-134a in micro-finned helically coiled tubes is given in Eq. (6) [46] whilst the two-phase frictional pressure drop was calculated through the use of the pressure drop multiplier as in Eq. (3).

$$\Delta P_{total,TP} = \Delta P_{f,TP} + \Delta P_{grav} + \Delta P_{mom,TP} \quad (6)$$

where:

$$\Delta P_{grav} = g \rho_l \tan \beta (1 - VF) \quad (7)$$

253
 254
 255
 256
 257
 258
 259
 260
 261
 262
 263
 264
 265
 266
 267
 268
 269
 270
 271
 272
 273
 274
 275
 276
 277
 278
 279
 280
 281
 282
 283
 284
 285
 286
 287
 288
 289
 290
 291
 292
 293
 294
 295
 296
 297
 298
 299

$$\Delta P_{mom,TP} = G^2 \left\{ \left[\frac{(1-x)^2}{\rho_l(1-VF)} + \frac{x^2}{\rho_v VF} \right]_{out} - \left[\frac{(1-x)^2}{\rho_l(1-VF)} + \frac{x^2}{\rho_v VF} \right]_{in} \right\} \quad (8)$$

Aria et al. [47]:

$$VF = \frac{x}{\rho_v} \left[(1 + 0.12(1-x)) \left(\frac{x}{\rho_v} + \frac{1-x}{\rho_l} \right) + \frac{1.18(1-x)[g\sigma(\rho_l - \rho_v)]^{0.25}}{G^2 \rho_l^{0.5}} \right]^{-1} \quad (9)$$

Cui et al. [46]

$$VF = \frac{1}{1 + 0.49 \chi_{tt}^{0.8036}} \quad (10)$$

Elsayed et al. [48]

$$VF = \frac{1}{\left[1 + 0.79 \left(\frac{1-x}{x} \right)^{0.78} \left(\frac{\rho_v}{\rho_l} \right)^{0.58} \right]} \quad (11)$$

Wongwises and Polsongkram [49]

$$VF = \frac{1}{1 + S \left(\frac{1-x}{x} \right) \frac{\rho_v}{\rho_l}} \quad (12)$$

Laohalertdecha and Wongwises [50]

$$VF = \left[1 + \frac{(1-x)}{x} \left(\frac{\rho_v}{\rho_l} \right)^{2/3} \right]^{-1} \quad (13)$$

The numerical models for the R-134a refrigerant frictional pressure drop in vertical helically coiled tubes as reported in the pertinent studies are a function of the Lockhart and Martinelli parameter, whilst the sole correlation for horizontal tubes is based on a numerical model by Kim et al. [51] for R-22 flow in coiled tubes. There is a general agreement that the higher mass fluxes and the vapour qualities increase the frictional pressure drop. These results are attributed to the higher vapour velocities which increase the shear stress at the interface of the vapour and the liquid. Furthermore, higher vapour qualities result in increased magnitudes of secondary flow which will result in higher degrees of entrainment and droplet redeposition, thus yielding greater flow turbulences [49]. Moreover, Lin and Ebadian [52] reported that when compared to the flow in the inner tube, the effects of the mass flux on the pressure drop were more significant in the annular section of the coil. These findings were attributed to the larger velocity and turbulence fluctuations of the refrigerant flowing in the annular section.

The effects of the coil geometry on the two-phase refrigerant frictional pressure drop were investigated by Scott Downing and Kojasoy [53] and Elsayed et al. [48]. For miniature diameter tubes, Downing and Kojasoy reported that when compared to single-phase flow, the curvature effects had a minimal impact on the frictional pressure drop. However, for small diameter tubes, Elsayed et al. reported that the frictional pressure drop is mainly a function of the tube diameter, with the pressure drop increasing with smaller tube diameters. The effect of the coil diameter was reported to be less significant. Elsayed et al. focused their study on the heat transfer characteristics and hence failed to provide a comprehensive analysis of their reported results.

When investigating the frictional pressure drop as a function of the heat flux, Wongwises and Polsongkram [54] reported that the heat flux had a minimal effect on the condensation frictional pressure drop. However, the evaporation frictional pressure drop was

300 reported to be a strong function of the heat flux [49]. This was attributed to the increase in the
 301 number of active nucleation sites on the tube wall which yielded higher bubble generation rates.
 302 The latter agitated the liquid film thus increasing the turbulence. Furthermore, the breaking of
 303 the bubbles at the liquid film surface induced the entrainment and redeposition of droplets
 304 which increased the shear stress. Kang et al. [11] and Wongwises and Polsongkram [49, 54]
 305 reported a decrease in the frictional pressure drop with higher wall temperatures. These results
 306 were attributed to the lower refrigerant viscosity and specific volume, which in turn resulted in
 307 a lower vapour velocity and shear stress between the vapour and liquid interface.

308 The sole study that investigated the frictional pressure drop of R-134a as a function of
 309 the coil orientation was reported by Lin and Ebadian [52] who concluded that the coil
 310 orientation resulted in an insignificant impact on the frictional pressure drop. The applications
 311 of micro-finned or corrugated helically coiled tubes were investigated by Cui et al. [46] and
 312 Laohalertdecha and Wongwises [50]. Both investigations reported correlations for the pressure
 313 drop multiplier based on the Lockhart and Martinelli numerical model for straight tubes.
 314 Moreover, both authors reported a significant increase in the frictional pressure drop (up to
 315 70%) over that of a smooth tube. Laohalertdecha and Wongwises attributed these results to the
 316 increased drag forces, the flow blockage due to the reduction in the tube cross-sectional area,
 317 the turbulence augmentation and the enhanced rotational flow reduction. The impact of the
 318 vapour quality and mass flux on the frictional pressure drop was similar to that reported for
 319 smooth tubes.

320

Authors	Helical coil design parameters	Principal experimental parameters	Quality	Main conclusions, proposed correlation and mean error
Miniature ($d_{it} < 1\text{mm}$)				
Scott Downing and Kojasoy (2002) [53]	234 < ID < 881 μm 2.80 < D < 7.94 mm	0.075 < δ_{it} < 0.3 0.62 < P < 1.4 M Pa $0 < q < 25$ 750 < G < 6330 500 < Re < 8000	0 < x < 0.9 Evaporation	Curvature effects have a minimal effect on the frictional pressure drop when compared to single-phase flow. where; $\phi_{l,tt}^2 = 1 + \frac{C}{\chi_{tt}} + \frac{1}{\chi_{tt}^2}$ $C = 3.598 \left(\frac{1}{\chi_{tt}} \right)^{0.012}$ ($\pm 15\%$)
Vertical orientation & Smooth tubes				
Kang et al. (2000) [11]	Tube-in-tube 12.7mm ID_{it} 21.2mm ID_{ot} $D=177.8\text{mm}$ Laminar & Turbulent	$\delta_{it}=0.075$ 100 < G < 400 $T=33^\circ\text{C}$ 1500 < Re < 900 0	0 < x < 1 Condensation	Very slow increase in the pressure drop with an increase in the mass flux. Pressure drop is a function of the cooling wall temperature, with a decrease in the pressure drop with an increase in the wall temperature. For $T_{wall} = 12^\circ\text{C}$, $\Delta P_{TP} = 14.2m_{ref}^{0.093}$ For $T_{wall} = 22^\circ\text{C}$, $\Delta P_{TP} = 4.2m_{ref}^{0.26}$ (-37.3% to 35.7%)
Han et al. (2005) [55]	Tube-in-tube 9.4mm ID_{it} 12.7mm OD_{it} 21.2mm ID_{ot} $D=177.8\text{mm}$	$\delta_{it}=0.053$ 100 < G < 420 $T_{sat}=35,40,46^\circ\text{C}$ 1500 < Re < 900 0	0 < x < 1 Condensation	Pressure drop increases with refrigerant mass flux. Frictional pressure drop is higher than that in a straight tube, whilst the effect of the mass flux on the pressure drop is more significant in straight tubes. No correlation provided
Wongwises and Polsong	Tube-in-tube 7.2mm ID_{it} 9.52mm OD_{it} 21.2mm ID_{ot}	$\delta_{it}=0.025$ $5 < q < 10$ 400 < G < 800	0.0 < x < 1 Evaporation	Increase in the frictional pressure drop with increasing quality, mass flux and heat flux. Marginal decrease with increasing saturation temperature.

kram (2006a) [49]	23.2mm OD_{ot} $D=305$ mm	$10 < T_{sat} < 20^{\circ}\text{C}$		$\phi_l^2 = 1 + \frac{13.37}{\chi_{tt}^{1.492}}$ <p>Used Ito's [6] correlation for the single-phase friction factor</p> <p>(±20%)</p>
Wongwises and Polsongkram (2006b) [54]	Tube-in-tube 8.3mm ID_{it} 9.52mm OD_{it} 21.2mm ID_{ot} 23.2mm OD_{ot} $D=305$ mm	$\delta_{it}=0.025$ $5 < q < 10$ $400 < G < 800$ $40 < T_{sat} < 50^{\circ}\text{C}$	$0.01 < x < 1$ Condensation	<p>Frictional pressure drop increases with average vapour quality and mass flux and decreases with increasing saturation temperature of condensation. Heat flux has a minimal effect on the pressure drop.</p> $\phi_l^2 = 1 + \frac{5.569}{\chi_{tt}^{1.492}} + \frac{1}{\chi_{tt}^2}$ <p>Used Ito's [6] correlation for the single-phase friction factor</p> <p>(±20%)</p>
El-Sayed Mossad et al. (2009) [56]	Tube-in-tube 7.39mm ID_{it} 9.54mm OD_{it} 16.92mm ID_{ot} 19.05mm OD_{ot} $D=216$ mm	$\delta_{it}=0.03$ $810 < P < 820$ kPa $2.5 < q < 12$ $95 < G < 710$ $1000 < Re < 14000$	$0.0 < x < 1$ Condensation	<p>Increase in the frictional pressure drop with the refrigerant mass flux.</p> <p>Pressure drop is significantly higher than in a straight tube.</p> <p>Used Han et al.'s [55] correlation</p>
Aria et al. (2012) [47]	Tube-in-tube 8.9mm ID_{it} 9.52mm OD_{it} 29mm ID_{ot} $D=305$ mm	$\delta_{it}=0.031$ $112 < G < 152$	$0.1 < x < 0.8$ Evaporation	<p>Pressure drop increases with higher inlet vapour quality and refrigerant mass flow rate. 150-220% higher than pressure drop in straight tubes.</p> <p>Used Wongwises and Polsongkram's [49] correlation for helical tubes</p> <p>(-73% to +39%)</p>
Micro-finned or corrugated tube				
Cui et al. (2008) [46]	Micro-finned 11.2mm ID 12.7mm OD $D=185$ mm Vertical	$\delta=0.061$ $0.5 < P < 0.58$ MPa $2.0 < q < 21.8$ $65 < G < 315$	$0.05 < x < 0.92$ Evaporation	<p>Two-phase pressure drop is greater than that in a straight pipe. Micro-fins also increase the pressure drop as does increasing mass flux and vapour exit quality.</p> <p>For Stratified flow:</p> $\phi_l^2 = 1 + \frac{48.2}{\chi_{tt}} + \frac{1}{\chi_{tt}^2}$ <p>For Annular flow:</p> $\phi_l^2 = 1 + \frac{59.8}{\chi_{tt}} + \frac{3.5}{\chi_{tt}^2}$ <p>Ito's [6] correlation for the single-phase friction factor was used</p> <p>(±20%)</p>
Laohalerdecha and Wongwises (2010) [50]	Corrugated $ID_{it}=8.7$ mm $OD_{it}=9.52$ mm $ID_{ot}=21.2$ mm $E=1.5$ mm Horizontal	$5 < q < 10$ $200 < G < 700$ $T_{sat}=40, 45, 50^{\circ}\text{C}$	$0.01 < x < 0.9$ Condensation	<p>Frictional pressure drop increases with refrigerant mass flux and quality. 70% increase in the frictional pressure drop over that of smooth tubes</p>

				$\phi_{l,tt}^2 = 1 + \frac{10}{\chi_{tt}} + \frac{1}{\chi_{tt}^2}$ <p style="text-align: center;">(±30%)</p>
Horizontal orientation & Smooth tubes				
Elsayed et al. (2012) [48]	1.1<ID<2.8mm 1.47<OD<4mm 30<D<60mm	0.037< δ <0.04 7 0.35<P<0.6M Pa 2.5<q<12 100<G<450	0.2<x<0.9 Evaporation	<p>Frictional pressure drop is a strong function of the inner tube diameter. The coil diameter has a marginal effect on the pressure drop.</p> <p>Kim et al.'s [51] correlation for R-22:</p> $\Delta P_{f,TP} = 2 \frac{f_{TP} G_{ref}^2}{\rho_l d_{it}} \left[1 + x \frac{\left(\frac{1}{\rho_v} - \frac{1}{\rho_l} \right)}{\frac{1}{\rho_v}} \right]$ <p>where:</p> $f_{TP} = 0.079 \left(\frac{G_{ref} d_{it}}{\mu_{TP}} \right)^{-0.25}$ $\mu_{TP} = \rho_{TP} \left[\frac{\chi \mu_v}{\rho_v} + \frac{(1-\chi)\mu_l}{\rho_l} \right]$ $\rho_{TP} = \rho_v VF + \rho_l (1-VF)$
Various orientations and smooth tube				
Lin and Ebadian (2007) [52]	Tube-in-tube 9.4mm ID _{it} 12.7mm OD _{it} 21.2mm ID _{ot} D=177.8mm Horizontal/45°/Vertical	$\delta_{it}=0.053$ 60<Re _{ref} <200 3600<Re _{wr} <22000 30<T _{ref} <35 16<T _{wr} <24	Condensation	<p>The effects of the tube orientation on the pressure drop were not significant whilst the effects of the refrigerant mass flow rate on the pressure drop were more significant in the annular section of the pipe when compared to the inner tube.</p> $\phi_l^2 = 1 - \frac{1.271}{\chi_{tt}^{1.492}} + \frac{1}{\chi_{tt}^2}$ <p style="text-align: center;">(±6%)</p>

Table 2: Review of experimental studies on the flow boiling/condensing frictional pressure drop characteristics of R-134a in helically coiled tubes

3. Gas-Water

In contrast to the paucity of studies on the gas-water two-phase flow heat transfer characteristics in helically coiled tubes [57], the open literature presents numerous studies on the two-phase gas-water pressure drop characteristics. Table 3 summarises the experimental studies and correlations for the frictional pressure drop with gas and water two-phase flow as presented in the pertinent literature. The majority of studies reviewed in this section have demonstrated a reasonable agreement with the original and modified Lockhart and Martinelli correlations. Some investigators have also reported the helix angle and the curvature ratio to have some impact on the frictional pressure drop whilst other investigators reported the frictional pressure drop to be independent of the latter design parameters. The effects of the air volumetric void fraction remain indeterminate due to conflicting results. As in the case of steam-water flow, the total two-phase pressure drop with air-water systems is calculated through Eq. (2) whilst the two-phase frictional pressure drop is calculated through the application of the pressure drop multiplier as in Eq. (3).

Most studies on the two-phase air-water flow in helically coiled tubes were developed for vertically orientated tubes. The earliest study was reported by Rippel et al. [58] who investigated annular, bubbly, slug, and stratified flows. In agreement with some studies reported for steam-water, they reported that the Lockhart and Martinelli correlation for

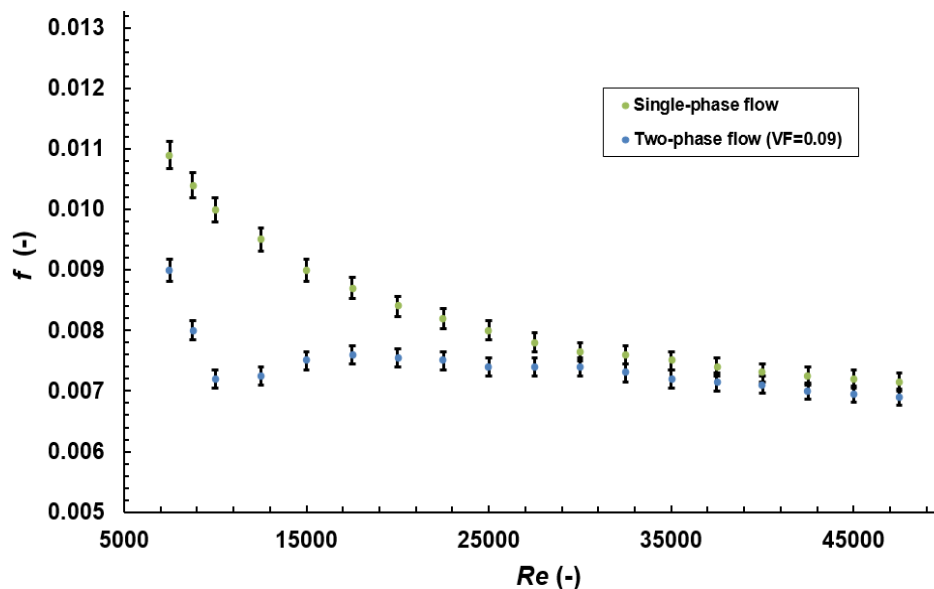
343 horizontal straight tubes predicted their data with reasonable accuracy. These results were
344 attributed to the fact that the Lockhart and Martinelli parameters are essentially ratios, while
345 the geometry of the tube does not impact on the ratio of the two-phase to single-phase pressure
346 drop given in Eq. (3). However, they also reported that the latter methodology also results in a
347 number of limitations, principally due to the fact that some pertinent factors that affect two-
348 phase flows are neglected. In view of this, Rippel et al. presented three empirical correlations
349 for the calculation of the two-phase flow pressure drop for annular, bubbly and stratified flows.
350 These correlations are based on the two-phase drag coefficient. Banerjee et al. [59] reported
351 similar results with the Lockhart and Martinelli correlation and presented modified equations
352 for the gas and liquid pressure drop multipliers, and the Lockhart and Martinelli parameter.
353 Banerjee were the first investigators to report that the helix angle did not have a significant
354 impact on the frictional pressure drop. Agakawa et al. [4] also reported a good agreement with
355 the Lockhart and Martinelli correlation whilst the frictional pressure drop was reported to be
356 independent of the coil curvature. They also presented two key empirical correlations to
357 calculate the ratios of the two-phase frictional pressure drop in the coil to those in a straight
358 tube and coil with liquid flow only. Xin et al. [8] presented a further development of the
359 Lockhart and Martinelli correlation whereby they included the effects of the three main forces
360 affecting the pressure drop these being: the inertia, liquid gravity and centrifugal forces. In fact,
361 they reported that the helix angle, coil diameter and pipe diameter had some effect on the
362 frictional pressure drop. Awwad et al. [20, 60] investigated the two-phase frictional pressure
363 drop in horizontal helically coiled tubes. Their conclusions and correlations are similar to those
364 presented by Xin et al. [8] for vertical tubes. Therefore, whilst being based on the original
365 Lockhart and Martinelli model, their correlations for horizontal coils included the effects of the
366 three principal forces affecting two-phase flow in coiled tubes.

367 Xin et al. [61] investigated the two-phase flow frictional pressure drop in annular
368 helicoidal pipes. As done in their earlier study [8] on vertical coils, they presented a correlation
369 for the calculation of the pressure drop multiplier which is a function of the Lockhart and
370 Martinelli parameter, as well as the Froude number. However, for the case of the annular tubes,
371 the latter is also a function of the inner and outer tube diameters. Vashisth and Nigam [62]
372 were the sole authors to investigate the frictional pressure drop in a coiled flow inverter. The
373 pressure drop was reported to be significantly higher than that for a straight helix. This result
374 was attributed to the higher recirculation rates and the complete flow inversion as a result of
375 the sudden shift in the flow direction. Vashisth and Nigam also reported that the Lockhart and
376 Martinelli correlation, both in its original and modified form, predicted their data for a very
377 limited range of flow rates. Therefore, they presented their own correlation for the two-phase
378 friction factor in a coiled flow inverter which is a strong function of the number of bends and
379 the curvature ratio. The latter was included due to their conclusions that smaller coil diameters
380 resulted in higher intensity secondary flows which consequently increased the two-phase
381 frictional pressure drop.

382 Chen and Guo [63] investigated the three phase oil-air-water flow in helically coiled
383 tubes. The frictional pressure drop was reported to be independent of the coil diameter whilst,
384 due to increased mixture viscosities, higher oil fractions resulted in higher pressure drops. A
385 correlation which is essentially a modified Chisholm correlation for straight tubes was also
386 presented. Chisholm's correlation was also used to correlate the data for sulphur hexafluoride-
387 water flow in helically coiled tubes [64]. The sole study in the pertinent literature that
388 investigated the gas-non-Newtonian pressure drop in helically coiled tubes was reported by
389 Biswas and Das [65]. They reported a large deviation with the Lockhart and Martinelli
390 correlation which was attributed to the non-Newtonian fluid properties. Therefore, they
391 presented an empirical correlation for the calculation of the friction factor which is a
392 function of the fluid and gas Reynolds number, the curvature ratio and fluid properties. In

393 agreement to pertinent conclusions made for gas-water flow [20, 59], the impact of the helix
 394 angle on the frictional pressure drop was also found to be negligible.

395 A recent study reported by Saffari et al. [17] investigated the frictional drag reduction
 396 through the use of two-phase bubbly flow in vertical helically coiled tubes. This study is based
 397 on earlier initiatives developed for straight tubes whereby two-phase bubbly flow resulted in a
 398 drag reduction over the corresponding single-phase flow [66, 67]. For turbulent flow with an
 399 air volumetric void fraction of 0.09, Saffari et al. reported a maximum drag reduction of 25%
 400 over that of single-phase flow, ceteris paribus (Fig. 4). The latter reduction was at its highest
 401 at the lower end of the turbulent flow Reynolds numbers. Saffari et al. attributed these results
 402 to the impact of the centrifugal force on the lighter phase, this being air, whereby due to their
 403 lighter density, bubbles accumulate on the tube inner wall in the flow boundary layer. At lower
 404 Reynolds numbers these bubbles are widely spread on the tube wall and consequently result in
 405 a significant reduction of the turbulent Reynolds stresses. Such results are in contrast to the
 406 findings reported in this section where all investigators reported frictional pressure drop
 407 multipliers in excess of 1.
 408



409 **Figure 4: Comparison of the friction factor for single-phase and two-phase flow in helically coiled tubes at**
 410 **a volumetric void fraction of 0.09 (Saffari et al. [17], Fig. 4)**
 411
 412
 413

Authors	Helical coil design parameters	Principal experimental parameters	Main conclusions, proposed correlation and mean error
Vertical orientation – Air-Water			
Rippel et al. (1966) [58]	$d=6.35\text{mm}$ $D=203\text{mm}$	$\delta=0.031$ $100 < Re < 15000$ Bubbly&Slug/Annular/Stratified	Data fitted the Lockhart-Martinelli parameter. Developed correlations based on the two-phase drag coefficient. Annular Flow: $\left(\frac{\Delta P}{\Delta L}\right)_{f,TP} = \left(\frac{\Delta P}{\Delta L}\right)_g + 4.44\varepsilon^{0.86} \left(\frac{\rho_g U^2}{gd}\right)$ Bubble and Slug Flow: $\left(\frac{\Delta P}{\Delta L}\right)_{f,TP} = \left(\frac{\Delta P}{\Delta L}\right)_g + 31.3\varepsilon^{1.25} \left(\frac{\rho_g U^2}{gd}\right)$ Stratified Flow: $\left(\frac{\Delta P}{\Delta L}\right)_{f,TP} = \left(\frac{\Delta P}{\Delta L}\right)_g + 3.2\varepsilon^{0.875} \left(\frac{\rho_g U^2}{gd}\right)$

Banerjee et al. (1969) [59]	15.34<d<54.8mm 152<D<610mm	0.108<δ<0.090 500<Re<40000	Helix angle had no significant effect on the frictional pressure drop. Data correlated well with the Lockhart and Martinelli correlation using the modified ϕ_l, ϕ_g and χ_{tt} : $\phi_l^2 = SF^{n-2} \left(\frac{d}{HD_l} \right)^{5-n}$ $\phi_g^2 = SF^{m-2} \left(\frac{d}{HD_g} \right)^{5-m}$ $\chi_{tt}^2 = \frac{\left(\frac{\Delta P}{\Delta z} \right)_l}{\left(\frac{\Delta P}{\Delta z} \right)_g}$ (±30%)
Akagawa et al. (1971) [4]	d=9.92mm D=109, 225 mm	0.044<δ<0.091 0<U _g <5m/s 0.35<U _l <1.16m/s Bubbly&Slug	Frictional pressure drop was measured as 1.1 to 1.5 times greater than that in straight tubes, ceteris paribus. Pressure drop is not a function of the curvature. Data fitted the Lockhart and Martinelli correlation. Empirical equations were also provided: $\frac{\Delta P_{f,TP,c}}{\Delta P_{f,TP,s}} = \frac{(1 + 144\delta^{1.61})}{Re_{TP}^{1.4\delta}}$ where: $Re_{TP} = \frac{U_l d}{(1 - VF_g)\mu_l}$ $\frac{\Delta P_{f,TP,c}}{\Delta P_{f,l,c}} = (1 - VF_g) \left[\left(\frac{2.3d}{D} \right)^{-1.4} \right]$ (±35%)
Kasturi and Stepanek (1971) [68]	d=12.5mm D=665 mm	δ=0.019 1E+3<De<1E+6 Stratified&Wavy	Data fitted the Lockhart-Martinelli parameter.
Whalley (1980) [69]	d=20.2mm D=1000mm B=6	δ=0.019 Stratified&Annular	Frictional pressure drop is the dominant pressure drop over the acceleration and gravity pressure drops. No correlation provided.
Rangachar yulu and Davies (1984) [70]	d=11,13mm 1.52<β<2.69	0.0427<δ<0.0541 1<vf _g <10 m ³ /h 0.04<vf _l <0.75 m ³ /h	Correlation also valid for air in glycerol and isobutyl alcohol solutions. $\phi_g - 1 = 0.05 Re_l \delta^{0.5} \left(\frac{U_{TP}}{CS} \right)^{-0.68} \left(\frac{\mu_l^4 g}{\rho_l \sigma_l^3} \right)^{0.18} \delta^{3.66}$
Xin et al. (1996) [8]	d=12.7,19.1,25.4,38 .1mm D=305,609 mm	0.02<δ<0.125 0.008<U _w <2.2 0.2<U _g <50 Bubbly flow	The helix angle, coil and pipe diameters have a marginal effect on the frictional pressure drop. For $F_d > 0.1$ $\phi_l = \left[1 + \frac{\chi}{434.6 F_d^{1.7}} \right] \left[1 + \frac{20}{\chi} + \frac{1}{\chi^2} \right]^{0.5}$ For $F_d \leq 0.1$ $\phi_l = \left[1 + \frac{\chi}{65.45 F_d^{0.6}} \right] \left[1 + \frac{20}{\chi} + \frac{1}{\chi^2} \right]^{0.5}$ where; $F_d = Fr \left(\frac{d}{D} \right)^{0.5} (1 + \tan\beta)^{0.2}$ $Fr = \frac{U_l^2}{gd}$

			(±35%)
Mandal and Das (2003) [15]	$d=10,13\text{mm}$ $131<D<2222\text{mm}$ $0<\beta<12$	$0.046<\delta<0.095$ $1.5<vf_g<52.5E-5$ $3.65<vf_l<14.2E-5$ $28<T_{mean}<32^\circ\text{C}$	The helix angle has no effect on the pressure drop. Empirical correlation was developed to calculate the two-phase friction factor. $f_{TP,l}$ $= 5.8853Re_l^{-1.1829\pm 0.0215} Re_g^{0.952\pm 0.0142} \left(\frac{\mu_l^4 g}{\rho_l \sigma_l^3}\right)^{0.022\pm 0.0086} \delta^{-0.282\pm 0.0369}$
Murai et al. (2006) [16]	$d=20\text{mm}$ $D=540,750\text{mm}$	$0.027<\delta<0.04$ $P=0.101\text{MPa}$ $1.76<U<5.28$ $15<T<17^\circ\text{C}$ $Re>10^4$ Bubbly/Plug/Slug flow	$\Delta P_{f,l} = f \rho_l (1 - VF) \frac{L U^2}{d^2}$ Used Ito's [6] correlation for the single-phase friction factor
Saffari et al. [17]	$d=12,19\text{mm}$ $D=200\text{mm}$	$0.06<\delta<0.095$ $P=0.101\text{MPa}$ $10000<Re<50000$ $0.03<VF<0.09$ Bubbly flow	25% reduction in the frictional pressure drop with $VF=0.09$ of air over that of single-phase flow, ceteris paribus. No correlation provided.
Horizontal orientation – Air-Water			
Awwad et al. (1995) [20]	$12.7<d<38.1\text{mm}$ $330<D<670\text{mm}$ $1<\beta<20$	$0.04<\delta<0.057$ $0.2<U_g<50\text{m/s}$ $0.008<U_l<2.2\text{m/s}$ Bubbly flow	Frictional pressure drop is a function of the flow rate of air and water and the Lockhart-Martinelli parameter. The helix angle has almost no effect on the frictional pressure drop whilst the tube and coil diameters have some effects which diminish at higher fluid flow rates. $\phi_l = \left[1 + \frac{\chi}{C(F_d)^{n1}}\right] \left[1 + \frac{12}{\chi} + \frac{1}{\chi^2}\right]^{0.5}$ where: $F_d \leq 0.3, C=7.79$ & $n1=0.576$ $F_d > 0.3, C=13.56$ & $n1=1.3$ (±32%)
Awwad et al. (1995) [60]	$d=25.4\text{mm}$ $D=350, 660\text{mm}$ $1<\beta<20$	$0.04<\delta<0.073$ $0.2<U_g<50\text{m/s}$ $0.008<U_l<2.2\text{m/s}$	Same conclusions as in Awwad et al. [20] $\phi_l = \left[\frac{\chi}{9.63F_d^{0.61}}\right] \left[1 + \frac{12}{\chi} + \frac{1}{\chi^2}\right]^{0.5}$ $F_d = Fr \delta^{0.1}$ (±35%)
Coiled flow inverter – Air-Water			
Vashisth and Nigam (2007) [62]	$5<d<15\text{mm}$	$0.05<\delta<0.149$ $8.33<vf_g<100E-5$ $3.33<vf_l<1000E-6$	Pressure drop increases by a factor of 1.2-2.5 more than that of a straight helix. Smaller coil diameters result in higher frictional pressure drops. $f_{TP} = \frac{29.4N^{0.16} \left(\frac{D}{d}\right)^{0.19} Re_g^{0.06}}{Re_l^{0.94}} \quad 400 < Re_l \leq 9000$ $f_{TP} = \frac{0.065N^{0.003} Re_g^{0.001}}{\left(\frac{D}{d}\right)^{0.003} Re_l^{0.13}} \quad Re_l \geq 10200$ (±15%)

Annular helicoidal tubes – Air-Water			
Xin et al. (1997) [61]	Tube-in-tube $OD_{it}=6.35, 9.525, 12.7$ mm $ID_{ot}=10.21, 15.748, 21.18$ mm $D=114.3, 177.8, 196.85$ mm Vertical and Horizontal orientations	$30 < Re_g < 30000$ $210 < Re_w < 23000$	Frictional pressure drop is a function of the flow rate of air and water and the Lockhart-Martinelli parameter, whilst the flow rate effect diminishes with an increase in the tube diameter. $\phi_l = \left[1 + \frac{0.0435 \chi^{1.5}}{F} \right] \left[1 + \frac{10.646}{\chi} + \frac{1}{\chi^2} \right]^{0.5}$ where; $F = Fr^{0.9106} e^{0.0458(\ln Fr)^2}$ $Fr = \frac{U_l^2}{g(ID_{ot} - OD_{it})}$
Three-phase: Oil-Air-Water			
Chen and Guo (1999) [63]	$d=39$ mm $D=265, 522.5$ mm $1 < \beta < 20$	$0.45 < U_g < 19.02$ m/s $0.018 < U_{wt} < 1.85$ m/s $0.0141 < U_o < 0.91$ m/s $15 < T_{mean} < 20$ °C $0.1 < P < 0.5$ MPa $VC_{oil} < 30\%$ $VC_w > 70\%$ Stratified/Oil-Droplet Stratified/Oil-Droplet/Annular Oil flow	The frictional pressure drop increases with the oil fraction in the mixture. Coil diameter has no effect on the frictional pressure drop. $\phi_l^2 = f(\theta) \left[1 - \frac{0.603}{\chi} + \frac{1}{\chi^2} \right]$ where: $f(\theta) = R^{0.0172} \left(\frac{1526}{G} \right)^{1.596} (\delta)^{0.175} \left(\frac{\mu_g \rho_o}{\mu_o \rho_o} \right)^{-1.238} \left(\frac{\mu_{wt} \rho_o}{\mu_o \rho_{wt}} \right)$ $R = \frac{U_g}{U_l}$ (±30%)
Gas-Non-Newtonian Fluid			
Biswas and Das (2008) [65]	$9.3 < d < 12$ mm $176.2 < D < 266.7$ m $0 < \beta < 12$ Vertical orientation	$0.035 < \delta < 0.09$ $0.44 < v_{fg} < 42.03$ E-5 $3.334 < v_{fi} < 15.00$ 3E-5 $28 < T_{mean} < 32$ °C $0.2 < MC < 0.8$	The effect of the helix angle on the pressure drop was negligible. Empirical correlation was developed to calculate the two-phase friction factor. $f_{TP,l}$ $= 0.4 Re_g^{0.757 \pm 0.025} Re_l^{-1.437 \pm 0.059} \left(\frac{\mu_{eff}^4 g}{\rho_l \sigma_l^3} \right)^{-0.348 \pm 0.017}$ $\delta^{0.721 \pm 0.076}$ (RE 8%)
SF6-Water			
Czop et al. (1994) [64]	$d=19.8$ mm $D=1170$ mm $\beta=7.27$	$\delta=0.017$ $0.1 < P < 1.35$ MPa $26000 < Re < 50000$ $500 < G < 3000$ Slug & Bubbly flow	Significant differences with the Lockhart-Martinelli correlation. Fairly good agreement with the Chisholm correlation [71]: $\phi_{l,tt}^2 = 1 + \frac{C}{\chi_{tt}} + \frac{1}{\chi_{tt}^2}$ where: $\chi_{tt} = \frac{1-x}{x} \left(\frac{\rho_g}{\rho_l} \right)^{0.5}$ $C = 1.5 \left[\left(\frac{\rho_g}{\rho_l} \right)^{0.5} + \left(\frac{\rho_l}{\rho_g} \right)^{0.5} \right]$

Table 3: Review of experimental studies on the air-water frictional pressure drop characteristics in helically coiled tubes

414
415
416
417
418
419

420 **4. Nanofluids**

421

422 *4.1. Experimental studies*

423

424 There is a significant paucity of studies on the pressure drop characteristics of
425 nanofluids in helically coiled or curved tube heat exchangers. Fakoor-Pakdaman et al. [72]
426 reported that the few studies reported on the investigation of nanofluid flow in helically coiled
427 tubes were mainly focused at investigating the heat transfer characteristics with the system
428 parameters. In fact, their study, published in 2013, was the first study to comprehensively
429 investigate the isothermal pressure drop with nanofluids in helically coiled tubes. As reported
430 in Section 1 of the present study, a number of authors have considered the ratio of the resultant
431 pressure drop with nanofluids in a helically coiled tube to that in a straight tube with the base
432 fluid only, to calculate the performance index given in Eq. (1). This is principally used to
433 appraise the application of heat transfer enhancement techniques as a function of the ratios of
434 the heat transfer coefficients and the pressure drops. The latter is particularly relevant to the
435 calculation of the heat exchanger performance, as the use of helical coils and nanofluids could
436 result in a significant increase in the pressure drop (circa 3.5 times) over that of the base fluid
437 in straight tubes [72].

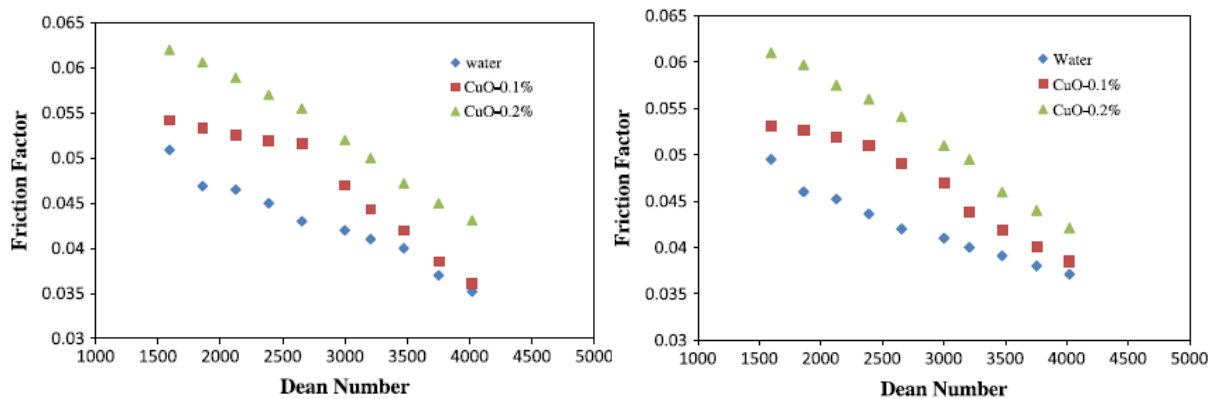
438 Table 4 summarises the pertinent experimental studies reviewed, categorised according
439 to the nanoparticles and the base fluids investigated. The principal nanoparticles which have
440 been reported by researchers are the oxides of copper and aluminium whilst the base fluids are
441 water and oil.

442 Most of the researches reviewed in the present study have reported an increase in the
443 nanofluid pressure drop with the nanoparticle concentration and the Reynolds number. This is
444 mainly attributed to the resultant higher relative mixture densities and viscosities [3, 73, 74].
445 However, most researchers agreed that at low fluid velocities the rate of increase in the pressure
446 drop with the nanoparticle volume concentration was smaller than that at higher fluid
447 velocities. Mukesh Kumar et al. [74] attributed this result to the dominance of the viscosity
448 effects at low Dean numbers. Furthermore, Hashemi and Akhavan-Behabadi [73] reported that
449 the higher rate of chaotic motion and migration of the nanoparticles at increased Reynolds
450 numbers could be the reason for the different rates of pressure drop increases. There are no
451 experimental studies which investigated the pressure drop characteristics of the principle
452 nanofluids, these being the oxides of aluminium and copper dispersed in water, at identical
453 system parameters. However, Hashemi and Akhavan-Behabadi reported that due to the
454 spherical properties of CuO nanoparticles, reduced levels of friction could result when
455 compared to other nanofluids. This is due to the rolling effect (instead of sliding) between the
456 oil and solid phases.

457 There is an agreement amongst authors [18, 14] that the transitional velocity, and hence
458 the critical Reynolds number of nanofluids will be higher than that of the base fluid. This is
459 due to the higher viscosity of the former. As reported in our review on the two-phase heat
460 transfer characteristics in helically coiled tubes [57] some controversies characterise the studies
461 on nanofluid flow in these tubes. The majority of investigations reviewed in the present study
462 reported a significant appreciation in the pressure drop with nanofluids over that of the base
463 fluid only. Furthermore, the increment in the pressure drop for helical tubes was reported to be
464 higher than that for straight pipes. In view of this, Suresh et al., Fakoor-Pakdaman et al. and
465 Kahani et al. [13, 72, 75] presented correlations for the calculation of the friction factor and
466 pressure drop with nanofluids. These correlations are principally a function of the coil
467 geometry, Dean or Reynolds numbers and the nanoparticle concentration. With a 2% weight
468 concentration of CuO nanoparticles in oil, flowing through a helically coiled tube, Hashemi
469 and Akhavan-Behabadi [73] reported an increase in the pressure drop of 20.3% over that of the

470 base fluid only whilst for a straight tube, this was measured as 13.2%. Similarly, for 0.2%
 471 volume concentration of CuO in water, Kannadasan et al. [18] reported that the friction factor,
 472 when compared to water flow only, increased by 24% and 23% for horizontal and vertical
 473 orientations respectively. However, in contrast to these findings, Suresh et al. and Wu et al.
 474 [75, 14] reported that the resultant pressure drop increment with a wide range of nanoparticle
 475 concentrations was marginal when compared to that of the base fluid alone. In fact, Wu et al.'s
 476 pressure drop results were reasonably predicted by the Ito [6] (laminar) and Seban and
 477 McLaughlin [76] (turbulent) equations for single-phase flow in helically coiled tubes. Suresh
 478 et al. attributed these results to the nanoscale size of the additive nanoparticles. Furthermore,
 479 whilst Wu et al. [14] reported that, due to their higher viscosity and density, nanofluids resulted
 480 in a mitigation of the secondary flow, Mukesh Kumar et al. [3] reported contradictory results.
 481 The latter results were attributed to the random motion of the nanoparticles which did not
 482 impede the formation of the secondary flow.

483 The nanofluid pressure drop as a function of the coil geometry was investigated by
 484 Kahani et al. [77] and Fakoor-Pakdaman et al. [72] who both reported lower pressure drops
 485 with a decrease in the curvature ratio. The pressure drop was also independent of the coil pitch.
 486 The former was principally attributed to the weaker centrifugal forces, hence minimising the
 487 effects of the secondary flow on the system pressure drop. The sole study which investigated
 488 the nanofluid pressure drop as a function of the helical coil orientation was reported by
 489 Kannadasan et al. [18]. They reported that the nanofluids in a vertical coil resulted in
 490 marginally lower pressure drop increments (over that of pure water) when compared to
 491 horizontal coils, ceteris paribus (Fig. 5). However, they failed to critically analyse these results.
 492



493
 494 **Figure 5: CFD simulation of the CuO nanoparticles in water, friction factor for: (a) Horizontal orientation (b) Vertical**
 495 **orientation (Kannadasan et al. [18], Figs. 7&8)**
 496
 497

Authors	Heat exchanger type/Flow regime	Nanofluid	Volume or weight conc.	Main conclusions, proposed correlation and mean error
Copper & Copper oxide nanoparticles & Water				
Akbaridoust et al. (2003) [78]	Laminar 200<Re<1000	Cu/H ₂ O	0.1-0.2% (VF)	The pressure drop increased with increasing particle volume concentration and mass flow rate. No correlation.
Suresh et al. (2011) [75]	Horizontal with smooth and dimpled surface Turbulent ID=4.85mm OD=6.3mm 2500<Re<6000	CuO/ H ₂ O	0.1-0.3% (VF)	Quasi no increase in the pressure drop with nanofluids over that with distilled water. $f = 0.1648Re^{0.97}(1 + VC)^{107.89} \left(1 + \frac{PR}{d}\right)^{-4.463}$ (±20%)

Kannadasan et al. (2012) [18]	Horizontal & vertical Turbulent $ID=9\text{mm}$ $OD=10.5\text{mm}$ $D=124\text{mm}$ $1600 < De < 4000$	CuO/ H ₂ O	0.1-0.2% (VC)	For both horizontal and vertical coils, an increase in the friction factor was measured with higher nanoparticle volume concentrations. Higher Dean numbers decreased the friction factor. For 0.2% volume concentration, the friction factor, when compared to water flow only, increased by 24% and 23% for horizontal and vertical orientations respectively. No correlation.
Copper oxide nanoparticles & Oil				
Hashemi and Akhavan-Behabadi (2012) [73]	Horizontal Laminar $ID=14.37\text{mm}$ $D=324\text{mm}$ $Re < 125$ $700 < Pr < 2050$	CuO/Oil	0.5-2% (WC)	The pressure drop increased with increasing particle volume concentration and Reynolds numbers. For 2% WC, the pressure drop, when compared to oil flow only, increased by 20.3%. For a straight tube this was measured as 13.2% No correlation.
Multi-Walled Carbon NanoTubes nanoparticles & Oil				
Fakoor-Pakdaman et al. (2012) [5]	Vertical Laminar $ID=15.6\text{mm}$ $220 < D < 320\text{mm}$ $100 < Re < 1800$	Multi-Walled Carbon NanoTubes/Oil	0.1-0.4% (WC)	Performance index, increases with higher nanoparticle weight concentrations. No correlation.
Fakoor-Pakdaman et al. (2013) [72]	Vertical Laminar $ID=15.6\text{mm}$ $220 < D < 320\text{mm}$ $10 < Re < 2000$	Multi-Walled Carbon NanoTubes/Oil	0.1-0.4% (WC)	The pressure drop increased with increasing particle volume concentration and mass flow rate. 31% pressure drop increase over the base fluid at the highest concentration. Pressure drop is independent of the coil pitch whilst a decrease in the curvature ratio results in a lower pressure drop. Pressure drop in the coiled tube is up to 2.5 times higher than that in a straight tube. $\frac{f_{TP}}{f_{bf}} = [1 + 0.031(\log Dn_m)^4](1 + 10WC)^{4.9}$ where: $Dn_m = Re \left\{ \delta^{-1} \left[1 + \left(\frac{p}{\pi D} \right)^2 \right] \right\}^{-0.5}$ (±20%)
Aluminium oxide & titanium dioxide nanoparticles & Water				
Kahani et al. (2013a) [13]	Horizontal Laminar $d=7\text{mm}$ $D=70, 140\text{mm}$ $500 < Re < 4500$ $5.89 < Pr < 8.95$ $115.3 < He < 1311.4$	Al ₂ O ₃ /H ₂ O TiO ₂ /H ₂ O	0.25-1.0% (VC)	The pressure drop increased with increasing particle volume concentration and mass flow rate. $\Delta P_{TP} = 5.584 He^{1.36} V F^{0.446} d^{0.163} R A^2$ where: $He = De \left[1 + \left(\frac{p}{2\pi D} \right)^2 \right]^{0.5}$
Kahani et al. (2013b) [77]	Horizontal Laminar $d=7\text{mm}$ $D=70, 140\text{mm}$ $500 < Re < 4500$ $5.89 < Pr < 8.95$ $115.3 < He < 1311.4$	Al ₂ O ₃ /H ₂ O	0.25-1.0% (VC)	The pressure drop increased with increasing particle volume concentration and mass flow rate. A decrease in the curvature ratio results in a lower pressure drop, whilst the coil pitch had a minimal effect on the pressure drop. No correlation.
Mukesh Kumar et al. (2013)	Laminar $5100 < Re < 8700$ $ID=9\text{mm}$	Al ₂ O ₃ /H ₂ O	0.1-0.8% (VC)	Generally, the pressure drop increased with increasing particle volume concentration and mass

[3]	$OD=10.5\text{mm}$ $D=93\text{mm}$			flow rate. Rate of pressure drop increase was higher when the Dean number increased. No correlation.
Wu et al. (2013) [14]	Double pipe Laminar & Turbulent $ID_{it}=13.28\text{mm}$ $ID_{ot}=26\text{mm}$ $D=254\text{mm}$ $800 < Re < 10000$	Al_2O_3 / H_2O	0.78-7.04% (WC)	Mitigation of secondary flow with nanofluids. Friction factor decreases with higher Reynolds numbers for laminar flow while it increases slowly for higher Reynolds numbers in turbulent flow. Their friction factor was predicted through the use of the Ito [6] (laminar) and Seban and McLaughlin [76] (turbulent) equations for single-phase flow. ($\pm 30\%$)
Mukesh Kumar et al. (2014) [74]	Laminar $0.03 < \dot{m} < 0.05$ $1600 < De < 2700$ $ID=10\text{mm}$ $OD=11.5\text{mm}$ $D=93\text{mm}$	Al_2O_3 / H_2O	0.1-0.8% (VC)	Generally, the pressure drop increased with increasing particle volume concentration and mass flow rate. Rate of pressure drop increase was higher when the Dean number increased. Hence, no significant increase in the pressured drop with 0.1% and 0.4% nanofluid particle volume concentration. No correlation.

498 **Table 4: Review of experimental studies of the pressure drop characteristics of nanofluids in helically coiled**
499 **tubes**

500

501 4.2 Numerical Studies

502

503 Research on the pressure drop and the general thermo-physical properties of nanofluids
504 in helically coiled heat exchangers is a relatively new development. In fact, the earliest research
505 in the pertinent literature was reported by Sasmito et al. [23] in 2011. The ANSYS Fluent
506 commercial software package was used in all of the studies reviewed and summarised in this
507 section. Therefore, the fluid flow and heat transfer governing equations, given in Eqs. (14-16),
508 were solved to measure the pressure drop and temperature distribution along the helically
509 coiled tubes.

510

511 Continuity:

512

$$513 \frac{\partial \rho}{\partial T} + \nabla \cdot (\rho V) = 0 \quad (14)$$

514

515 Momentum:

516

$$517 \rho \frac{\delta V}{\delta T} + \nabla \cdot \tau_{ij} - \nabla P + \rho FB = 0 \quad (15)$$

518

519 Energy:

520

$$521 \rho \frac{De}{\delta T} + \rho(\nabla \cdot V) = \frac{\partial Q}{\partial T} - \nabla \cdot Q + \phi_d \quad (16)$$

522

523 where V is the fluid velocity, FB are the body forces, ϕ_d is the energy dissipation term and Q is
524 the heat transfer by conduction. The numerical analysis studies reviewed in this section
525 assumed that the nanofluid flow through the tubes is incompressible, single-phase and fully
526 developed, both hydrodynamically and thermally. The SIMPLEC algorithm was used by a
527 number of studies to solve the flow field [21, 31], whilst for turbulent flow modelling, the
528 Standard Turbulence $k-\varepsilon$ model as proposed by Launder and Spalding, was used [79]. The

529 thermo-physical properties of the nanofluids were obtained using the equations given in Eqs.
530 (17-28) [21, 31].

531
532 Density:

$$534 \rho_{nf} = (1 - VF)\rho_{bf} + VF\rho_{np} \quad (17)$$

535
536 Heat capacity:

$$538 (\rho C_p)_{nf} = (1 - VF)(\rho C_p)_{bf} + VF(\rho C_p)_{np} \quad (18)$$

539
540 Effective thermal conductivity:

$$542 k_{eff} = k_{static} + k_{Brownian} \quad (19)$$

543
544 Static thermal conductivity:

$$546 k_{static} = k_{bf} \left[\frac{k_{np} + 2k_{bf} - 2(k_{bf} - k_{np})VF}{k_{np} + 2k_{bf} + (k_{bf} - k_{np})VF} \right] \quad (20)$$

547
548 Brownian thermal conductivity:

$$550 k_{Brownian} = 5E4\beta VF \rho_{bf} C_{p,bf} \sqrt{\frac{\kappa T}{2\rho_{np} r d_{np}}} f(T, VF) \quad (21)$$

551
552 where the Boltzmann constant, $\kappa = 1.3807E-23$ J/K

553
554 Modelling function for CuO, $1\% \leq VF \leq 6\%$, β :

$$556 \beta = 9.881(100VF)^{-0.9446} \quad (22)$$

557
558 Modelling function for Al₂O₃, $1\% \leq VF \leq 10\%$, β :

$$560 \beta = 8.4407(100VF)^{-1.07304} \quad (23)$$

561
562 Modelling function for ZnO, $1\% \leq VF \leq 7\%$, β :

$$564 \beta = 8.4407(100VF)^{-1.07304} \quad (24)$$

565
566 Modelling function for SiO₂, $1\% \leq VF \leq 10\%$, β :

$$568 \beta = 1.9526(100VF)^{-1.4594} \quad (25)$$

569
570 Modelling function, $f(T, VF)$:

$$572 f(T, VF) = (2.8217E - 2)VF + (3.917E - 3) \left(\frac{T}{T_o} \right) + (VF(-3.0699E - 2) - (3.91123E - 3)) \quad (26)$$

573
574 Dynamic viscosity:

575

$$\frac{\mu_{eff}}{\mu_{bf}} = \frac{1}{1 - 34.87 \left(\frac{d_{inp}}{d_{bf}} \right)^{-0.3} VF^{1.03}} \quad (27)$$

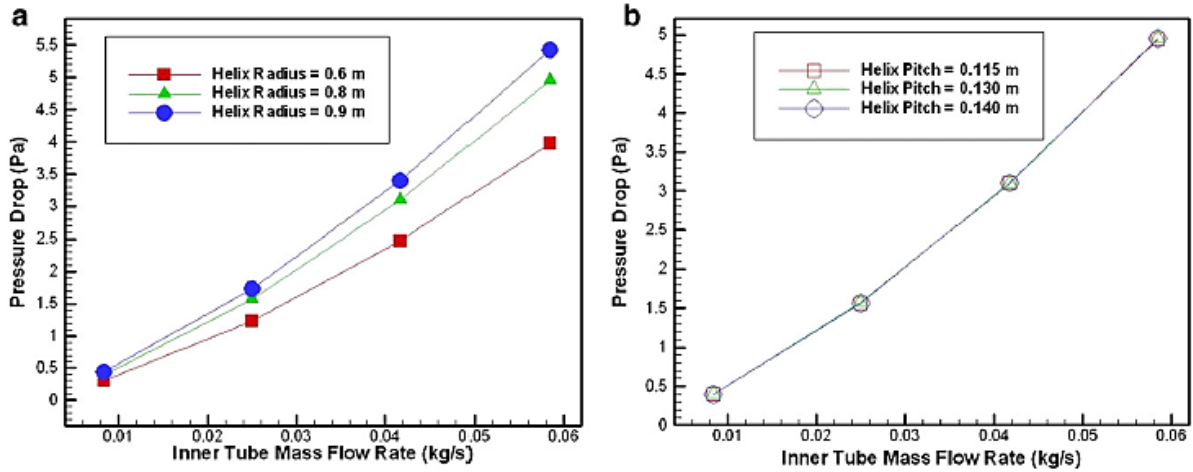
577 where the equivalent diameter of the base fluid molecule is:
578
579

$$d_{i_{bf}} = \left(\frac{6M}{N\pi\rho_{bf}} \right) \quad (28)$$

581 Table 5 summarises the numerical studies on the pressure drop characteristics with nanofluid
582 laminar and turbulent flow in helically coiled tubes. The studies summarised in this section are
583 in reasonable agreement with the data reported in the experimental studies reviewed in Section
584 4.1. Furthermore, some controversy also characterises the reviewed numerical studies. Hence,
585 whilst a number of authors [21, 22, 80] reported an increase in the frictional pressure drop with
586 higher nanoparticle volume concentrations as well as higher nanofluid pressure drops over that
587 of the base fluid only, Sasmito et al. [23] reported that at a nanoparticle volume concentration
588 of 1%, the calculated pressure drop was lower than that for pure water. Sasmito et al. attributed
589 these results to the fact that at low volume concentrations, the nanoparticles have a minimal
590 effect on the fluid viscosity, whereas the temperature effects on the nanofluid thermo-physical
591 properties are more significant. Intriguingly, Aly [30] also reported that the aluminium oxide
592 nanoparticles with a maximum volume concentration of 2% did not result in an increase to the
593 resultant pressure drop. Therefore, their data was in reasonable agreement with the single-phase
594 friction factor correlations by Mishra and Gupta and Ito [7, 6]. Similar results were also
595 reported by Suresh et al. and Wu et al. [75, 14] through their experimental investigations. One
596 of the advantages of numerical simulations is the minimal cost incurred for each simulation.
597 Hence, Narrein and Mohammed [21] were able to investigate the flow characteristics of a
598 combination of oil, ethylene glycol and water based nanofluids. They reported that due to the
599 high viscosities of oil based nanofluids, the latter resulted in the highest calculated pressure
600 drop when compared to ethylene glycol and water based nanofluids. Narrein and Mohammed
601 also reported higher pressure drops with decreasing nanoparticle diameters which were more
602 intense at higher fluid velocities. These results were attributed to the resultant increase in the
603 fluid viscosity which could result in higher wall shear stresses.
604

605 Through their numerical investigations, Elsayed et al. [29] and Moraveji and Hejazian
606 [80] presented correlations for the prediction of the friction factor. The former's correlation
607 takes the form of a ratio of the nanofluid flow pressure drop in a helically coiled tube to that in
608 a straight tube, *ceteris paribus*. This correlation is a function of the fluid properties, represented
609 through a modified Reynolds number and the tube geometry, represented through the curvature
610 ratio. The correlation presented by the latter authors is markedly different as it is not a function
611 of the coil geometry. In fact, it is a sole function of the fluid properties, represented through
612 the nanoparticle volume concentration and the Reynolds number.

613 Mohammed and Narrein [31] and Aly [30] investigated the nanofluid pressure drop
614 characteristics with the coil geometry. In agreement with the experimental results reported by
615 Kahani et al. [13] and Fakoor-Pakdaman et al. [5], an increase in the nanofluid frictional
616 pressure drop was reported with a reduction in the coil diameter, whilst the pressure drop
617 decreased with larger tube diameters. As reported in Section 4.1, these results can be attributed
618 to the reduction in the centrifugal forces with larger helix diameters. As illustrated in Fig. 6,
619 the pressure drop was also reported to be independent of the helix pitch.



620
621 **Figure 6: CFD simulation of the CuO nanoparticles in water, pressure drop for: different helix radii (a), pitches (b)**
622 **(Mohammed and Narrein [31], Fig. 7a&b)**
623
624

Authors	Heat exchanger type / Flow regime	Nanofluid	Volume or Weight Concentration	Main conclusions, proposed correlation and mean error
Sasmito et al. (2011) [23]	Square tubes Laminar	Al ₂ O ₃ /H ₂ O CuO/H ₂ O	0-1% (VC)	Helical coil resulted in the highest pressure drop when compared to straight, conical and in-plane coiled tubes. At 1% nanoparticle concentration, the pressure drop was lower than that for water. No correlation.
Jamshidi et al. (2012) [22]	Laminar 1700 < Re < 2500	Al ₂ O ₃ /H ₂ O	1-3% (VC)	Friction factor increased with higher nanoparticle volume concentrations and lower Reynolds numbers. No correlation.
Mohammed and Narrein (2012) [31]	Laminar 0.01 < ṁ < 0.06 d=32,42,52mm D=600,800,900 mm	CuO/H ₂ O	4% (VC)	Pressure drop increased with a reduction in the coil diameter and decreased with larger tube diameters. No correlation.
Narrein and Mohammed (2013) [21]	Laminar 0.01 < ṁ < 0.06	CuO/H ₂ O/Engine Oil/Ethylene glycol Al ₂ O ₃ /H ₂ O/Engine Oil/Ethylene glycol ZnO/H ₂ O/Engine Oil/Ethylene glycol SiO ₂ /H ₂ O/ Engine Oil/Ethylene glycol	1-4% (VC)	Due to the different densities, SiO ₂ had the highest pressure drop followed by Al ₂ O ₃ , ZnO, CuO. Due to higher viscosities, pressure drop increased with higher nanoparticle concentrations and decreasing nanoparticle diameters. Due to higher wall shear stresses this effect is more intense at higher fluid velocities. Pressure drop for oil based nanofluids resulted in the highest pressure drop followed by ethylene glycol and water based nanofluids. No correlation.

Elsayed et al. (2014) [29]	Turbulent 20000 < Re < 50000	Al ₂ O ₃ /H ₂ O	0-3% (VC)	Pressure drop in coils with nanofluids was measured as a ratio to that of water in a straight tube. $\frac{f_{nf,c}}{f_{bf,s}} = \frac{f_{nf,c}}{f_{nf,s}} = \frac{4(0.08Re_{nf}^{-0.25} + 0.012\delta^{0.5})}{0.316Re_{nf}^{-0.25}}$ (±5%)
Aly (2014) [30]	Tube-in-tube Turbulent D=180,240,300m m 2 < v _{fi} < 5LPM 10 < v _{fi} < 25LPM	Al ₂ O ₃ /H ₂ O	05-2% (VC)	Single-phase friction factor correlations by Ito and Mishra and Gupta are also valid for nanofluids. Friction factor increased with curvature ratios. No pressure drop increase with nanoparticle volume concentration. No correlation.
Moraveji and Hejazian (2014) [80]	Laminar d=14.4mm D=324mm	CuO/Oil	0.5-2% (WC)	Pressure drop with 2% nanoparticles is 11% higher than that for the base fluid, ceteris paribus. Pressure drop for the base fluid in the helical coil was 3 times higher than that in a straight tube. $f = 1.9254Re^{-1.223}(1 + VC)^{0.00781}$ (±15%)

Table 5: Review of numerical studies on the pressure drop characteristics of nanofluids in helically coiled tubes

5. Scope for further research

As discussed in Section 3, recent studies have suggested that the introduction of small air bubbles ($b < 0.5\text{mm}$) in turbulent flow could result in a substantial reduction of the frictional pressure drop over that of pure water. A number of studies have investigated this concept for two-phase flow in straight tubes [66, 67] whilst Saffari et al. [17] presented the sole study for helically coiled tubes. Saffari et al.'s conclusions are in substantial disagreement with the findings reported by the majority of investigations on air-water two-phase flow, where the introduction of the second phase was reported to enhance the frictional pressure drop. In fact, the pressure drop multiplier in Eq. (3), as originally defined by Lockhart and Martinelli, was typically reported to be in excess of unity. Such evident controversies should be addressed through further research on the frictional pressure drop due to bubbly air-water two-phase flows in coiled tubes.

As reported in a study published by one of the authors of the present study [81], air-water two-phase flow through helically coiled tube heat exchangers characterises many modern condensing sealed heating systems. Bubbly flow finds its origins in the supersaturated conditions at the heat exchanger wall. Whilst numerous studies investigated the air-water bubbly flow pressure drop, these studies were developed through the insertion of artificial bubbles. This presents significant scope for further research on the bubbly flow two-phase frictional pressure drops, where bubbles nucleate and detach at the tube wall and therefore, the volumetric void fraction at the return and flow ends of the heat exchanger would be dissimilar. Moreover, in view of the fact that numerous studies have suggested enhanced heat transfer coefficients with the addition of nanoparticles to water [75, 18], there is scope for further research on the three-phase air-water-nanoparticles frictional pressure drop in helically coiled tube heat exchangers.

Due to the recent development of nanofluids as a means for the enhancement of the fluid heat transfer characteristics, there is ample scope for further research in this field of study. The majority of the pertinent studies available in the open literature have focused their

656 investigations on the resultant heat transfer characteristics. This is evidenced by the paucity of
657 correlations presented for the calculation of the frictional pressure drop when compared to
658 those available for the heat transfer coefficient [57]. Further investigations should be developed
659 to address the conflicting results for the impact of the nanoparticle concentration on the
660 frictional pressure drop as outlined in Section 4. Studies should also be developed for the
661 purpose of investigating the frictional pressure drop as a sole function of the type of
662 nanoparticles. Such studies are deemed necessary in view of the conclusions made by Hashemi
663 and Akhavan-Behabadi [73] who reported that due to their typical spherical shape, copper
664 oxide nanoparticles could yield lower frictional pressure drops. The open literature presents a
665 single study on the two-phase frictional pressure drop as a function of the coil orientation [18],
666 where horizontal coils were reported to yield marginally higher pressure drops. However, the
667 authors failed to provide a detailed appraisal for the latter results. Furthermore, this study was
668 developed with copper oxide nanoparticles in water and hence, further studies are required to
669 investigate the impact of the coil orientation with widely used nanoparticles and base fluids,
670 such as aluminium oxide and oil respectively. Moreover, the pertinent literature failed to
671 comprehensively investigate the distribution of the secondary phase (nanoparticles) in coiled
672 tubes. Therefore, whilst Wu et al. [14] reported that nanofluid flow in coiled tubes did not yield
673 a significant phase separation, no other relevant studies investigated this pertinent flow
674 characteristic. Such avenues for future fundamental research will complement and facilitate the
675 research and development of high efficiency heat exchangers as well as open new opportunities
676 for industry-led heat exchanger tube design initiatives, whereby the distribution of the
677 secondary phase could be manipulated for optimised system efficiencies.

678

679 **6. Conclusions**

680

681 This paper has provided a review on all the investigations available in the pertinent literature
682 on the two-phase pressure drop characteristics in helically coiled tubes. Therefore the relevant
683 investigations on steam-water flow boiling, R-134a evaporation and condensation, air-water
684 flow and nanofluids have been critically reviewed. The correlations for the calculation of the
685 frictional two-phase pressure drop were also tabulated with the corresponding system
686 parameters. Whilst being more complex than single-phase flow, two-phase flow is more
687 relevant to numerous engineering applications. Therefore a comprehensive understanding of
688 the two-phase pressure drop is necessary to ensure that no excessive, energy consuming,
689 pumping power is required. The pertinent conclusions outlined in the current study can be
690 summarised through the following points:

691

692 • For steam-water flow boiling, the frictional pressure drop increases with the vapour
693 quality and mass flux whilst it decreases with higher system pressures. The appreciation
694 of the frictional pressure drop with the vapour quality is more significant at qualities
695 below 0.3. The curvature ratio does not appear to have a significant influence on the
696 two-phase flow boiling frictional pressure drop multiplier whilst there is some
697 controversy surrounding the influence of the coil orientation and heat flux. Some
698 studies have correlated their data to widely cited correlations for straight tubes such as
699 those given by: Lockhart and Martinelli, Martinelli and Nelson and Chen.

700 • For R-134-a evaporation and condensation in helically coiled tubes, the curvature ratio
701 appears to have some impact on the resultant frictional pressure drop for R-134a flow
702 in non-miniature helically coiled tubes ($d > 1\text{mm}$). The pertinent investigations have also
703 concluded that the frictional pressure drop increases with higher vapour qualities and
704 refrigerant mass fluxes, whilst the tube orientation has no significant impact on the

705 pressure drop. The majority of the correlations presented are a function of the Lockhart
706 and Martinelli parameter.

- 707 • The pertinent literature presents numerous correlations for the prediction of the two-
708 phase frictional pressure drop with air-water bubbly flow. The majority of
709 investigations have correlated their data using the original or modified Lockhart and
710 Martinelli correlation for straight tubes, whilst other authors presented their own
711 empirical correlations. The early investigations reported the two-phase pressure drop to
712 be independent of the coil design parameters such as the curvature ratio and the helix
713 angle, whilst more recent studies have suggested a marginal impact on the two-phase
714 pressure drop by the latter parameters. The frictional pressure drop as a function of the
715 air volumetric void fraction remains indeterminate due to conflicting results.
- 716 • Few correlations are available to calculate the frictional pressure drop with nanofluids.
717 The majority of experimental and numerical investigations on nanofluids flowing in
718 helically coiled tubes have reported a significant increment (up to 3.5 times) in the
719 frictional two-phase pressure drop over that of pure water in straight tubes. Such
720 conclusions were mainly attributed to the higher relative mixtures and densities as well
721 as the secondary flow formed in curved tubes. Due to the dominance of the viscosity
722 effects at low fluid velocities, the impact of the nanoparticle concentration on the two-
723 phase frictional pressure drop is stronger at higher Reynolds numbers. The frictional
724 pressure drop was also reported to be a function of the curvature ratio and the coil
725 orientation with marginally larger pressure drops for horizontal coils. Controversy
726 surrounds the impact of nanofluids on the frictional pressure drop, where some
727 investigations reported a decrease in the resultant pressure drop while other studies
728 reported the pressure drop to be quasi-identical to that with pure water in coiled tubes.
729

730 This paper has also outlined areas for further research, principally in the fields of air-water and
731 nanofluids two-phase flows and three-phase air-water-nanoparticles flow. Such studies could
732 take the form of fundamental research as well as industrial research and development initiatives
733 with the aim of enhancing the system efficiencies through the reduction of the two-phase
734 pressure drop.

735 **Acknowledgments**

736 The authors of the current investigation would like to thank the University of Central
737 Lancashire UK, for facilitating the completion of this study as well as the various authors who
738 have been contacted during the course of this study.
739

740 **Notation List**

741		
742		
743		
744	<i>A</i>	Heat transfer area (m ²)
745	<i>b</i>	Bubble diameter (m)
746	<i>bf</i>	Base fluid (-)
747	<i>c_p</i>	Specific heat (J/kgK)
748	<i>C</i>	Constant depending on the flow condition of the vapour and liquid i.e. 5 for laminar 749 and 20 for turbulent flows (-)
750	<i>CS</i>	Stratified speed of sound (m/h)
751	<i>d</i>	Tube diameter (m)
752	<i>D</i>	Helix diameter (m)
753	<i>De</i>	Dean number (-)
754	<i>Di</i>	Diameter of nanoparticle (m)

755	E	Corrugation depth (m)
756	f	Friction factor (-)
757	Fr	Froude number (-)
758	FB	Body forces (N)
759	g	Acceleration due to gravity (m/s)
760	G	Mass flux (kg/m ² s)
761	h^*	Mean heat transfer coefficient after applying enhancement techniques (Nanoparticles
762		and helical coils) (W/m ² K)
763	h_{st}	Mean heat transfer coefficient inside a straight tube with base fluid only
764	He	Helical coil number (-)
765	H	Coil vertical height (m)
766	HD	Hydraulic diameter (m)
767	ID	Inner tube diameter (m)
768	k	Thermal conductivity (W/mK)
769	L	Length (m)
770	\dot{m}	Mass flow rate (kg/s)
771	M	Molecular weight (mol/g)
772	MC	Mass concentration (kg/m ³)
773	N	Number of bends (-)
774	OD	Outside tube diameter (m)
775	p	Pitch (m)
776	P	System pressure (-)
777	Pr	Prandtl number (-)
778	PI	Performance index (-)
779	PR	Pitch ratio (-)
780	ΔP^*	Mean pressure drop after applying enhancement techniques (Nanoparticles and helical
781		coils) (Pa)
782	ΔP_{st}	Mean pressure drop inside a straight tube with base fluid only (Pa)
783	ΔP_{TP}	Two-phase frictional pressure drop (Pa)
784	q	Heat flux (kW/m ²)
785	Q	Heating power (kW)
786	rd	Radius of nanoparticle (m)
787	Re	Reynolds number (-)
788	RA	Adjusted correlation coefficient (-)
789	RE	Average relative error (%)
790	RMS	Root mean square (-)
791	S	Slip ratio (-)
792	SF	Shape factors (-)
793	T	Temperature (⁰ C)
794	U	Superficial velocity (m/s)
795	v	Specific volume (m ³ /kg)
796	vf	Volume flow rate (m ³ /s)
797	V	Flow velocity (m/s)
798	VC	Volume concentration (-)
799	VF	Void fraction (-)
800	WC	Mass concentration as fraction (-)
801	x	Steam quality (-)
802	z	Vertical elevation (m)
803		
804		

805 **Greek symbols**

806

- 807 β Helix angle ($^{\circ}$)
 808 γ Friction factor multiplier (-)
 809 δ Curvature ratio: Internal tube radius d_i /mean coil radius D (-)
 810 ε Volumetric quality, liquid volume flow rate to total volume flow rate (-)
 811 η Performance index (-)
 812 κ Boltzmann constant (J/K)
 813 μ Dynamic viscosity (Pa/s)
 814 ρ Density (kg/m^3)
 815 σ Surface tension (N/m)
 816 τ Sheer stress (N/m^2)
 817 ϕ_d Dissipation term (m^2/s^3)
 818 ϕ_l Two-phase multiplier (-)
 819 χ Lockhart-Martinelli parameter (-) $\chi = \left(\frac{1-x}{x}\right)^{0.9} \left(\frac{\rho_g}{\rho_l}\right)^{0.5} \left(\frac{\mu_l}{\mu_g}\right)^{0.1}$
 820 ψ The unevenness correction factor (-)

821

822 **Subscripts**

823

- 824 *Acc* Acceleration
 825 *bf* Base fluid
 826 *c* Coil
 827 *crit* Critical
 828 *eff* Effective
 829 *f* Frictional
 830 *g* Gas properties/flow
 831 *grav* Gravity
 832 *g,tt* Gas phase turbulent flow
 833 *it* Inner tube
 834 *l* Liquid properties/flow
 835 *l,tt* Liquid phase turbulent flow
 836 *m* Mixture
 837 *n* nth
 838 *nf* Nanofluid
 839 *np* Nanoparticle
 840 *NS* No slip conditions
 841 *o* Oil
 842 *ot* Outer tube
 843 *ref* Refrigerant side
 844 *s* Straight tube
 845 *sat* Saturation conditions
 846 *st* Single-phase conditions
 847 *TP* Two-phase conditions
 848 *tt* Turbulent liquid and vapour flow
 849 *v* Vapour
 850 *v,tt* Vapour phase turbulent flow
 851 *wt* Water

852

853

854 **Reference List**

855
856
857
858
859
860
861
862
863
864
865
866
867
868
869
870
871
872
873
874
875
876
877
878
879
880
881
882
883
884
885
886
887
888
889
890
891
892
893
894
895
896
897
898
899
900

1. Goering D.J., Humphrey J.A.C, Greif R., 1997, The dual influence of curvature and buoyancy in fully developed tube flows, *International Journal of Heat and Mass Transfer*, 40, pp. 2187-2199
2. Pabhanjan D.G., Raghavan G.S.V., Rennie T.J., 2002, Comparison of heat transfer rates between a straight tube heat exchanger and a helically coiled heat exchanger, *Int. Comm. Heat Mass Transfer*, 29 (2) pp. 185-191
3. Mukesh Kumar P.C., Kumar J., Suresh S., 2013, Experimental investigation on convective heat transfer and friction factor in a helically coiled tube with Al₂O₃/water nanofluid, *Journal of Mechanical Science and Technology*, 27 (1), pp. 239-245
4. Akagawa K., Tadashi S., Minoru U., 1971, Study on a gas-liquid two-phase flow in helically coiled tubes, *Bulletin of JSME*, 14 (72), pp. 564-571
5. Fakoor-Pakdaman M., Akhavan-Behabadi M.A., Razi P., 2012, An experimental investigation on thermo-physical properties and overall performance of MWCNT/heat transfer oil nanofluid flow inside vertical helically coiled tubes, *International Journal of Thermal Sciences*, 40, pp. 103-111
6. Ito H., 1959, Friction factors for turbulent flow in curved pipes, *ASME Journal of Basic Engineering*, 81, pp. 123-134
7. Mishra P., Gupta S.N., 1979, Momentum transfer in curved pipes 1, Newtonian fluids, *Industrial Engineering Chemical Processes Design and Development*, 18, pp. 130-137
8. Xin R.C., Awwad A., Dong Z.F., Ebadian M.A., 1996, An investigation and comparative study of the pressure drop in air-water two-phase flow in vertical helicoidal pipes, *International Journal of Heat Transfer*, 39 (4), pp. 735-743
9. Campolumghi F., Cumo M., Ferrari G., and Palazzi G., 1977, Full scale tests and thermal design for coiled once-through heat exchangers, *American Institute of Chemical Engineers Symposium Series*, 73, pp. 215-222
10. Nariai H., Kobayashi M., Matsuoka T., 1982, Friction pressure drop and heat transfer coefficient of two-phase flow in helically coiled tube once-through steam generator for integrated type marine water reactor, *Journal of Nuclear Science and Technology*, 19 (11), pp. 936-947
11. Kang H.J., Lin C.X., Ebadian M.A., 2000, Condensation of R134a flowing inside helicoidal pipe, *International Journal of Heat and Mass Transfer*, 43 pp. 2553-2564
12. Han J.T., Lin C.X., Ebadian M.A., 2005, Condensation heat transfer and pressure drop characteristics of R-134a in an annular helical pipe, *International Communications in Heat and Mass Transfer*, 32, pp. 1307-1316
13. Kahani M., Heris S.Z., Mousavi S.M., 2013, Comparative study between metal oxide nanopowders on thermal characteristics of nanofluid flow through helical coils, *Powder Technology*, 246, pp. 82-92
14. Wu Z., Wang L., Sunden B., 2013, Pressure drop and convective heat transfer of water and nanofluids in a double-pipe helical heat exchanger, *Applied Thermal Engineering*, 60, pp. 266-274
15. Mandal S.N., Das S.K., 2003, Gas-liquid flow through coils, *Korean Journal of Chemical Engineering*, 20(4), pp. 624-630
16. Murai Y., Yoshikawa S., Toda S., Ishikawa M., Yamamoto F., 2006, Structure of air-water two-phase flow in helically coiled tubes, *Nuclear Engineering and Design*, 236, pp. 94-106

- 901 17. Saffari H., Moosavi R., Gholami E., Nouri N.M., 2013, The effect of bubble in the
902 pressure drop reduction in helical coil, *Experimental Thermal and Fluid Science*, 51,
903 pp. 251-256
- 904 18. Kannadasan N., Ramanathan K., Suresh S., 2012, Comparison of heat transfer and
905 pressure drop in horizontal and vertical helically coiled heat exchanger with Cu/water
906 based nanofluids, *Experimental Thermal and Fluid Science*, 42, pp. 64-70
- 907 19. Nouri N.M., Motlagh S.Y., Navidbakhsh M., Dalilhaghi M., Moltani A.A., 2013,
908 Bubble effect on pressure drop reduction in upward pipe flow, *Experimental Thermal
909 and Fluid Science*, 44, pp. 592-598
- 910 20. Awwad A., Xin R.C., Dong Z.F., Ebadian M.A., Soliman H.M., 1995, Measurement
911 and correlation of the pressure drop in air-water two-phase flow in horizontal helicoidal
912 pipes, *International Journal of Multiphase Flow*, 21 (4), pp. 607-619
- 913 21. Narrein K., Mohammed H.A., 2013, Influence of nanofluids and rotation on helically
914 coiled tube heat exchanger performance, *Techmochimica Acta*, 564, pp. 13-23
- 915 22. Jamshidi N., Farhadi M., Sedighi K., Domeiry G., 2012, Optimisation of design
916 parameters for nanofluids flowing inside helical coils, *International Communications
917 in Heat and Mass Transfer*, 39, pp. 311-317
- 918 23. Sasmito P.A., Kurnia J.C., Mujumdar A.S., 2011, Numerical evaluation of laminar heat
919 transfer enhancement in nanofluid flow in coiled square tubes, *Nanoscale Research
920 letters*, 6:376
- 921 24. Naphon P., Wongwises S., 2006, A review of flow and heat transfer characteristics in
922 curved tubes, *Renewable and Sustainable Energy Reviews*, 10 (5), pp. 463-490
- 923 25. Guo L.J., Feng Z.P., Chen X.J., 2001, Pressure drop oscillation of steam-water two-
924 phase flow in a helically coiled tube, *International Journal of Heat and Mass Transfer*,
925 44, pp. 1555-1564
- 926 26. Cioncolini A., Santini L., Ricotti M.E., 2008, Subcooled and saturated water flow
927 boiling pressure drop in small diameter helical coils at low pressure, *Experimental and
928 Fluid Science*, 32 pp. 1301-1312
- 929 27. Zhao L., Guo L., Bai B., Hou Y., Zhang X., 2003, Convective boiling heat transfer and
930 two-phase flow characteristics inside a small horizontal helically coiled tubing once-
931 through steam generator, *International Journal of Heat and Mass Transfer*, 46 pp. 4779-
932 4788
- 933 28. Kozeki M., Nariai H., Furukawa T., Kurosu K., 1970, A study of helically coiled tube
934 once-through steam generator, *Bull.JSME*, 13(66), pp. 1485-1494
- 935 29. Elsayed A., Al-dadah R., Mahmoud S., Rezk A., 2014, Numerical investigation of
936 turbulent flow heat transfer and pressure drop of Al₂O₃/Water nanofluid in helically
937 coiled tubes, *International Journal of Low-Carbon Technologies*, 0, pp. 1-8
- 938 30. Aly W., 2014, Numerical study on turbulent heat transfer and pressure drop of
939 nanofluid in coiled tube-in-tube heat exchangers, *Energy Conversion and Management*,
940 79, pp. 304-316
- 941 31. Mohammed H.A., Narrein K., 2012, Thermal and hydraulic characteristics of nanofluid
942 flow in a helically coiled tube heat exchanger, *International Communications in Heat
943 and Mass Transfer*, 39, pp. 1375-1383
- 944 32. Bi Q.C., Chen T.K., Luo Y.S., Zheng J.X., Jing J.G., Frictional pressure drop of steam-
945 water two-phase flow in helical coils with small helix diameter, in: Chen et al. (Eds.),
946 Proc. Of the 3rd International Symposium on Multiphase Flow and Heat Transfer, vol.
947 1, Xi'an Jiaotong Univ. Press and Begell House Inc., 1994, pp. 498-505
- 948 33. Owhadi A., Bell K.J., Crain Jr. B., 1968, Forced convection boiling inside helically
949 coiled tubes, *International Journal of Heat and Mass Transfer*, 11, pp. 1179-1793

- 950 34. Lockhart, R.W., Martinelli, R.C.; 1949, Proposed correlation of data for isothermal
951 two-phase two-component flow in pipes, *Chemical Engineering Progress*, 45, pp. 39–
952 48
- 953 35. Martinelli R.C., Nelson D.B., 1948, Prediction of pressure drop during forced
954 circulation boiling of water, *Transactions of ASME*, 70, pp. 695-702
- 955 36. Chen L., Steam-water two-phase flow frictional pressure drop in straight tubes, in: Chen
956 X. (Ed.), *Selected papers of multiphase flow and heat transfer*, Paper 7, Xi'an Jiaotong
957 University Press, 1982, pp. 7.1-7.6
- 958 37. Guo L., Feng Z., Chen X., 2001, An experimental investigation of the frictional
959 pressure drop of steam-water two-phase flow in helical coils, *International Journal of*
960 *Heat and Mass Transfer*, 44, pp. 2601-2610
- 961 38. Santini L., Cioncolini A., Lombardi C., Ricotti M., 2008, Two-phase pressure drops in
962 a helically coiled steam generator, *International Journal of Heat and Mass Transfer*, 51,
963 pp. 4926-4939
- 964 39. Ruffell A.E., The application of heat transfer and pressure drop data to the design of
965 helical coil once-through boilers, *Symposium on multi-phase flow systems*, University
966 of Strathclyde, Institute of Chemical Engineering Symposium Series, 38, Paper 15
- 967 40. Unal H.C., van Gasselt M.L.G., van't Vertlaat P.M., 1981 Dryout and two-phase flow
968 pressure drop in sodium heated helically coiled steam generator tubes at elevated
969 pressures, *International Journal of Heat and Mass Transfer*, 24, pp. 285-298
- 970 41. Chen X.J., Zhou F.D., 1981, An investigation of flow pattern and frictional pressure
971 drop characteristics of air-water two-phase flow in helical coils, in: *Proceedings of the*
972 *Fourth Miami International Conference on Alternate Energy Sources*, pp. 120-129
- 973 42. Guo L.J., Chen S.K., Zhang Z.P., Correlation for predicting pressure drop of single and
974 two-phase flow through horizontal helically coiled tubes, in: *Proceedings of the Third*
975 *International Symposium on Multiphase Flow and Heat Transfer*, Xi'an, China, 1994,
976 pp. 514-521
- 977 43. Kubair V.G., 1986, Heat transfer to multiphase flow in coiled pipes, *Heat Transfer*, C.L.
978 Tien et al. (Ed.), *Proceedings of the 8th International Heat Transfer Conference*, San
979 Francisco USA, 5, pp. 2355-2360
- 980 44. Ju H., Huang Z., Xu Y., Duan B., Yu Y., 2001, Hydraulic performance of small bending
981 radius helical coil-pipe, *Journal of Nuclear Science and Technology*, 38 (10), pp. 826-
982 831
- 983 45. Tong L.S., Weisman J., 1996, *Thermal analysis of pressurised water reactors*. 3rd
984 edition, American Nuclear Society
- 985 46. Cui W., Li L., Xin M., Jen T.C., Chen Q., Liao Q., 2006, A heat transfer correlation of
986 flow boiling in micro-finned helically coiled tube, *International Journal of Heat and*
987 *Mass Transfer*, 49, pp. 2851-2858
- 988 47. Aria H., Akhavan-Behabadi M.A., Shemirani F.M., 2012, Experimental Investigation
989 of flow boiling heat transfer and pressure drop of HFC-134a inside a vertical helically
990 coiled tube, *Heat Transfer Engineering*, 33(2), pp. 79-86
- 991 48. Elsayed, A.M., Al-Dadah R.K., Mahmoud S., Rezk A., 2012, Investigation of flow
992 boiling heat transfer inside small diameter helically coiled tubes, *International Journal*
993 *of Refrigeration*, 35, pp. 2179-2187
- 994 49. Wongwises S., Polsongkram M., 2006a, Evaporation heat transfer and pressure drop of
995 HFC-134a in a helically coiled concentric tube-in-tube heat exchanger, *International*
996 *Journal of Heat and Mass Transfer*, 49, pp. 658-670
- 997 50. Laohalertdecha S., Wongwises S., 2010, The effects of corrugation pitch on the
998 condensation heat transfer and pressure drop of R-134a inside horizontal corrugated
999 tube, *International Journal of Heat and Mass Transfer*, 53 pp. 2924-2931

- 1000 51. Kim J.W., Kim J.H., Seo S.K., Kim J.H., Kim J.S., 2000, Characteristics of heat transfer
1001 and pressure drop of R-22 inside an evaporating tube with small diameter helical coil,
1002 Transactions of the Korean Society of Mechanical Engineers Series, B24 (5), pp. 699-
1003 708
- 1004 52. Lin C.X., Ebdian M.A., 2007, Condensation heat transfer and pressure drop of R-134a
1005 in annular helicoidal pipe at different orientations, International Journal of Heat and
1006 Mass Transfer, 50 pp. 4256-4264
- 1007 53. Scott Downing R., Kojasoy G., 2002, Single and two-phase pressure drop
1008 characteristics on miniature helical channels, Experimental Thermal and Fluid Science,
1009 26 pp. 535-546
- 1010 54. Wongwises S., Polsongkram M., 2006b, Condensation heat transfer and pressure drop
1011 of HFC-134a in a helically coiled concentric tube-in-tube heat exchanger, International
1012 Journal of Heat and Mass Transfer, 49, pp. 4386-4398
- 1013 55. Han J.T., Lin C.X., Ebdian M.A., 2005, Condensation heat transfer and pressured drop
1014 characteristics of R-134a in an annular helical pipe, International Communications in
1015 Heat and Mass Transfer, 32, pp. 1307-1316
- 1016 56. El-Sayed Mosaad M., Al-Hajeri M., Al-Ajmi R., Koliub A.M., 2009, Heat transfer and
1017 pressure drop of R-134a condensation in a coiled, double tube, Heat Mass Transfer, 45
1018 pp. 1107-1115
- 1019 57. Fsadni A.M., Whitty J.P.M., 2016, A review of the two-phase heat transfer
1020 characteristics in helically coiled tube heat exchangers, International Heat and Mass
1021 Transfer, 95, pp. 551-565
- 1022 58. Rippel G.R., Edit C.M., Jordan H.B., 1966, Two-phase flow in a coiled tube, Industrial
1023 and Engineering Chemistry Process Design and Development, 5 (1) pp. 32-39
- 1024 59. Banerjee S., Rhodes E., Scott D.S., 1969, Studies on cocurrent gas-liquid flow in
1025 helically coiled tubes, The Canadian Journal of Chemical Engineering, 47, 445-453
- 1026 60. Awwad A., Xin R.C., Dong Z.F., Ebdian M.A., Soliman H.M., 1995, Flow patterns
1027 and pressure drops in air/water two-phase flow in horizontal pipes, Journal of Fluids
1028 Engineering, 117(4), pp. 720-726
- 1029 61. Xin R.C., Awwad A., Dong Z.F., Ebdian M.A., 1997, An experimental study of single-
1030 phase and two-phase flow in annular helicoidally pipes, National Heat Transfer
1031 Conference, 8, pp. 11-17
- 1032 62. Vashisth S., Nigam K.D.P., 2007, Experimental Investigation of Pressure Drop during
1033 Two-Phase Flow in a Coiled Flow Inverter, Industrial & Engineering Chemistry
1034 Research, 46 (14) pp.5043-5050
- 1035 63. Chen X., Guo L., 1999, Flow patterns and pressure drop in oil-air-water three-phase
1036 flow through helically coiled tubes, International Journal of Multiphase Flow, 25, pp.
1037 1053-1072
- 1038 64. Czop V., Barbier S., Dong S., 1994, Pressure drop, void fraction and shear stress
1039 measurements in an adiabatic two-phase flow in a coiled tube, Nuclear Engineering and
1040 Design, 149 pp. 323-333
- 1041 65. Biswas A.B., Das S.K., 2008, Two-phase frictional pressured drop of gas-non-
1042 Newtonian liquid flow through helical coils in vertical orientation, Chemical
1043 Engineering and Processing, 47 pp. 816-826
- 1044 66. Mazzitelli I., Lohse D., Toschi F., 2003, The effect of micro bubbles on developed
1045 turbulence, Physics of Fluids, 15(1), L5
- 1046 67. Bao-Guo C., Nan-Sheng L., 2011, Direct numerical simulations of turbulent channel
1047 flows with consideration of the buoyancy effect of the bubble phase, Journal of
1048 Hydrodynamics, 23 (3), pp. 282-288

- 1049 68. Kasturi G., Stepanek J.B., 1972, Two-phase flow-I. Pressure drop and void fraction
1050 measurements in concurrent gas-liquid flow in a coil, *Chemical Engineering Science*,
1051 27 pp. 1871-1880
- 1052 69. Whalley P.B., 1980, Air-water two-phase flow in a helically coiled tube, *International*
1053 *Journal of Multiphase flow*, 6(4), pp. 345-356
- 1054 70. Rangacharyulu K., Davies G.S., 1984, Pressure drop and holdup studies of air-liquid
1055 flow in helical coils, *The Chemical Engineering Journal*, 29 pp. 41-46
- 1056 71. Chisholm D., 1967, Pressure gradients during the flow of incompressible two-phase
1057 mixtures through pipes, Venturis and orifice plates, *Chemical Engineering*, 12(9), pp.
1058 1368-1371
- 1059 72. Fakoor-Pakdaman M., Akhavan-Behabadi M.A., Razi P., 2013, An empirical study on
1060 the pressure drop characteristics of nanofluid flow inside helically coiled tubes,
1061 *International Journal of Thermal Sciences*, 65, pp. 206-213
- 1062 73. Hashemi S.M., Akhavan-Behabadi M.A., 2012, An empirical study on heat transfer and
1063 pressure drop characteristics of CuO-base oil nanofluid flow in a horizontal helically
1064 coiled tube under constant heat flux, *International Communications in Heat and Mass*
1065 *Transfer*, 39, pp. 144-151
- 1066 74. Mukesh Kumar P.C., Kumar J., Sendhilnathan S., Tamilarasan R., Suresh S., 2014,
1067 Heat transfer and pressure drop of Al₂O₃ nanofluid as coolant in shell and helically
1068 coiled tube heat exchanger, *Bulgarian Chemical Communications*, 46(4) pp. 743-749
- 1069 75. Suresh S., Chandrasekar M., Chandra Sekhar S., 2011, Experimental studies on heat
1070 transfer and friction factor characteristics of CuO/water nanofluid under turbulent flow
1071 in a helically dimpled tube, *Experimental Thermal and Fluid Science*, 35, pp. 542-549
- 1072 76. Seban R.A., McLaughlin E.F., 1963, Heat transfer in tube coils with laminar and
1073 turbulent flow, *International Journal of Heat and Mass Transfer*, 6, pp. 387-395
- 1074 77. Kahani M., Zeinali Heris S., Mousavi S.M., 2013, Effects of curvature ratio and coil
1075 pitch spacing on heat transfer performance of Al₂O₃/Water nanofluid laminar flow
1076 through helical coils, *Journal of Dispersion Science and Technology*, 34:12, pp. 1704-
1077 1712
- 1078 78. Akbaridoust F., Raksha M., Abbassi A., Saffar-Avval M., 2013, Experimental and
1079 numerical investigation of nanofluid heat transfer in helically coiled tubes at constant
1080 wall temperature using dispersion model, *International Journal of Heat and Mass*
1081 *Transfer*, 58, pp. 480-491
- 1082 79. Rabienataj Darzi A.A., Farhadi M., Sedighi K., Aallahyari S., Aghajani Delavar, 2013,
1083 Turbulent heat transfer of Al₂O₃ – water nanofluid inside helically corrugated tubes:
1084 Numerical Study, *International Communication in Heat and Mass Transfer*, 41, pp. 68-
1085 75
- 1086 80. Moraveji M.K., Hejazian M., 2014, CFD examination of convective heat transfer and
1087 pressure drop in a horizontal helically coiled tube with CuO/Oil base nanofluid,
1088 *Numerical Heat Transfer, Part A: Applications*, 66 pp. 315-329
- 1089 81. Fsadni A.M., Ge Y.T., Lamers A.G., 2011, Measurement of bubble detachment
1090 diameters from the surface of the boiler heat exchanger in a domestic central heating
1091 system, *Applied Thermal Engineering*, 31, (14-15), pp. 2808-2818
1092